Met.O.809

METEOROLOGICAL OFFICE

Scientific Paper No. 29

An Investigation of Air Motion in Frontal Precipitation

by T. W. HARROLD, B.Sc., D.I.C. and J. M. NICHOLLS, B.Sc.

LONDON: HER MAJESTY'S STATIONERY OFFICE

PRICE 6*s.* 6*d.* NET

Met.O.809

METEOROLOGICAL OFFICE

Scientific Paper No. 29

An Investigation of Air Motion in Frontal Precipitation

by T. W. HARROLD, B.Sc., D.I.C. and J. M. NICHOLLS, B.Sc.

LONDON

HER MAJESTY'S STATIONERY OFFICE

1968

U.D.C. 551·501·81:
551·515·827:
551·558·29

Contents

Summary 1

Introduction 1

Method and accuracy of analysis 2

Case studies 7

Comparison of case studies 40

Conclusion 45

Acknowledgements 45

Bibliography 46

An Investigation of Air Motion in Frontal Precipitation

by T. W. Harrold, B.Sc., D.I.C. and J. M. Nicholls, B.Sc.

SUMMARY

Measurements of horizontal and vertical air motions in six cases of frontal precipitation are presented. The observations were made using a pulsed Doppler radar at Pershore, Worcestershire. It was found that variations of the horizontal wind field over tens of minutes were generally small, implying only small mesoscale fluctuations. The maximum vertical wind shear was often very similar to that reported by radiosonde stations about 150 kilometres away. Two régimes of vertical air motion occurred. When the frontal zone was well above the ground the rate of ascent or descent was tens of centimetres per second, but as the front lowered more variable structures with velocities in excess of 1 metre per second were observed. In the cases most representative of the usual frontal situation in Britain, i.e. a front approaching from the west, descent predominated beneath the frontal zone. Vertical velocities were also calculated from relative-flow wet-bulb potential temperature (θ_w) charts. These provided a clear picture of the presence of moist tongues of air in frontal zones on the synoptic scale, but generally underestimated, by a factor of two or more, the magnitude of the vertical velocity during the precipitation.

1. INTRODUCTION

This paper presents the results of several case studies of horizontal divergence and both horizontal and vertical air motion in frontal precipitation. The main observational tool is the pulsed Doppler radar located at Pershore, Worcestershire. Several workers, for example Probert-Jones and Harper,[1]* have used such a radar pointing vertically to estimate vertical air motion in showers. Lhermitte and Atlas[2] showed that the radar can also be used to estimate accurately the horizontal wind and Caton[3] outlined a method of determining the horizontal divergence and hence vertical velocity of the airflow in steady precipitation. Harrold[4] and Browning[5] assessed the errors involved in such measurements and each presented a case study. Although the individual radar measurements of divergence are made over a small area (less than 300 km^2 in the present study) the broad features of the observations, especially when averaged over tens of minutes, seem representative of an area possibly ten times larger than this.

The radar measurements are made from a fixed point. Variations in time can be converted to spatial variations by assuming that the pattern moves at a constant speed—that of the synoptic features. In the absence of marked topographical effects, averaging the measurements over several hours should enable synoptic-scale motions to be determined. However, the data are of equal interest on the mesoscale. Conventional radar plan position indicator displays of frontal precipitation show that rainfall rates vary over distances of tens of kilometres, implying significant atmospheric structure on this scale. A Doppler radar is at present the most practical means of investigating changes in air motion on this scale.

* The superscript figures refer to the bibliography on p. 46.

The aims of the present paper are as follows:

(i) To describe the air motion during a number of occasions of frontal precipitation and to compare the mesoscale structure with the air motion indicated by isentropic analyses on the synoptic scale.

(ii) To determine any features common to most or all of the case studies.

The method and accuracy of the analysis is described in the next section. Much of this is a summary of the description given by Harrold[4] and is included here for completeness. Paragraphs 2.5. and 2.6. describe the format of the presentation of each case study and summarize the days for which data are available. Each case study is then presented separately. In the final sections (3.1. *et seq.*) of the paper the studies are compared and some general conclusions drawn.

2. METHOD AND ACCURACY OF ANALYSIS

2.1. *The Doppler radar*

The 3·2-cm pulsed Doppler radar at Pershore has been described by Boyenval[6] and also by Caton.[7] The beam width is 1½° to the half-power points and the pulse length is 0·8 microseconds, so, for example, at a range of 2 km a volume of about $2{\cdot}5 \times 10^6$ m³ is sampled. The radial velocities of targets (in this case precipitation) are determined from the Doppler frequency shift of the returned signal. The information is produced in discrete form and is displayed as a matrix, each row corresponding to a range interval along the beam of about 140 m and each column to a velocity interval of either 0·5 or 1·0 m/s. Photographs of the display have been published by Boyenval,[6] Caton,[7] Probert-Jones[8] and Probert-Jones and Harper.[1]

2.2. *Measurement of horizontal wind and divergence*

If the horizontal wind at a point of measurement has speed u and direction α, the velocity V measured toward the radar is

$$V = u\cos(\alpha-\phi)\cos\varepsilon + w\sin\varepsilon = u_\phi\cos\varepsilon + w\sin\varepsilon \qquad \ldots(1)$$

where ϕ and ε are the azimuth and elevation respectively of the beam, w is the vertical velocity of the precipitation and u_ϕ is the horizontal wind component in direction ϕ. Measurements of V are taken at 15° intervals of azimuth throughout a 360° rotation (taking about 1½ minutes) at a constant elevation angle. In a uniform wind field the wind speed is given by

$$u = \frac{1}{12\cos\varepsilon}\sqrt{\left\{\left(\sum_1^{24} V\cos\phi\right)^2 + \left(\sum_1^{24} V\sin\phi\right)^2\right\}} \qquad \ldots(2)$$

(where the summation is taken over the 24 measurements taken at 15° intervals of ϕ)

and the direction by $\alpha = \frac{\pi}{2} - \tan^{-1}\frac{\Sigma V\cos\phi}{\Sigma V\sin\phi}$.

Typically the probable error in these quantities is less than ±0·25 m/s and ±1°.

If D is the horizontal divergence (+ve) or convergence (−ve) and r is the radius of the circle of observation at any one height then

$$\pi r^2 D = -2\pi r\frac{\sum_1^{24} u_\phi}{24}. \qquad \ldots(3)$$

Therefore from (1) and (3)

$$D = \frac{-\sum_{1}^{24} u_\phi}{12r} = \frac{24w \sin \varepsilon - \sum_{1}^{24} V}{12r \cos \varepsilon}.$$

The expression for D contains the fall-speed w of the precipitation. This is measured with the aerial pointing vertically and it is assumed that this value is applicable to the circle of observation at any one height. At the elevation angles used in this study (15° and 30°), this assumption restricts the applicability of the method to study of precipitation in which there are no localized updraughts or downdraughts in excess of about 0·3 m/s. An alternative procedure would have been to use smaller elevation angles (so that $w \sin \varepsilon$ could be neglected) but because of the limited sensitivity of the radar this would have restricted the height to which measurements could be made.

The probable error in a single measurement of D was assessed by Harrold[4]—the results being summarized in Figure 1 of that paper. At a given angle of elevation and height the error is less in snow than in rain because the narrower spectrum of velocities in snow simplifies the estimation of w. Assuming no change of w around the circle of observation, at any one height the magnitude of the error in D decreases as the area of the circle of observation increases, since the error is inversely proportional to this area. On the other hand, as the circle of observation increases there is more likelihood of the overhead value of w not being representative of the entire circle, but it is believed that this error has been minimized by estimating divergence only when the overhead value of w is steady over tens of minutes.

Browning[5] considered an additional error resulting from the axis of the radar not being vertical, so that the angle of elevation varied systematically during the rotation. This kind of error might be quite serious in the presence of vertical wind shear. It is not thought that this error is significant in the present study since the verticality of the axis was checked by rotating the aerial through 360° of azimuth at an elevation of 90°. If the aerial axis was inclined at 0·2° to the vertical during the rotation, a horizontal wind of 25 m/s would shift the velocity spectrum through about 0·2 m/s, which would have been noticeable on the display. No shift was observed, which indicates that the aerial axis was vertical to within 0·2°.

2.3. *Measurement of vertical velocity*

Vertical velocity can be estimated either from the divergence measurements or, if the velocity was more than about 0·5 m/s, from the observations obtained at the times when the aerial was vertical.

(i) *Divergence measurements.* Vertical velocities are calculated from the divergence measurements using the continuity equation

$$\omega = -\int_p D \, \mathrm{d}p$$

where ω is the vertical air velocity (mb/s) and p is the pressure. The error in ω results almost entirely from the error in D. As an example of the magnitude of this error, in snow above 2 km and at an elevation angle of 15° the probable error in the change in ω over a height interval of 150 m is less than 2×10^{-4} mb/s (about 0·2 cm/s). In computing ω, errors from successive heights are accumulated. Figure 1 shows the probable error in vertical velocity, relative to that at 600 m, calculated on alternative assumptions that errors from successive

height ranges are either random or systematic. The actual probable error lies between the two curves for a given elevation. Errors at an elevation of 15° in rain (not shown) are similar to those in snow at 30°; those in rain at 30° are excessive and are excluded. Errors arising from successive rotations of the aerial are probably random so that vertical velocities meaned over several rotations are more accurate than those shown in Figure 1.

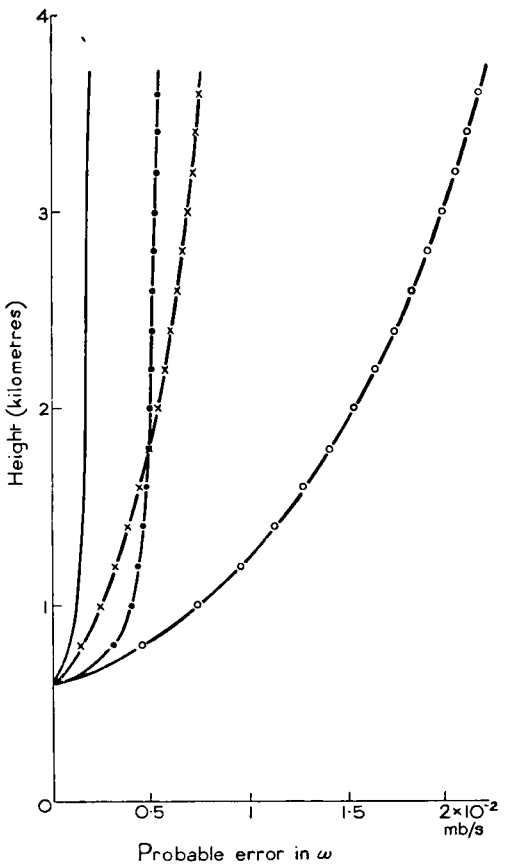

FIGURE 1. Probable error in vertical air velocity (ω), relative to the velocity at 600 m, calculated from radar measurements of horizontal divergence in snow.

c———o Aerial elevation 30°, errors from successive heights assumed systematic
·— — —· Aerial elevation 30°, errors from successive heights assumed random
x———x Aerial elevation 15°, errors from successive heights assumed systematic
— — — Aerial elevation 15°, errors from successive heights assumed random

Figure 2 shows an example of the volume sampled during a series of 30° rotations in a pattern moving at 60 km/h, the rotations being repeated every 6 minutes. It can be seen in this example that circles of observation at any one height overlap above 1·8 km, whereas below this height they are independent. In practice, velocity profiles were often averaged over both 15° and 30° rotations so that the volume sampled was less simple than that indicated in Figure 2.

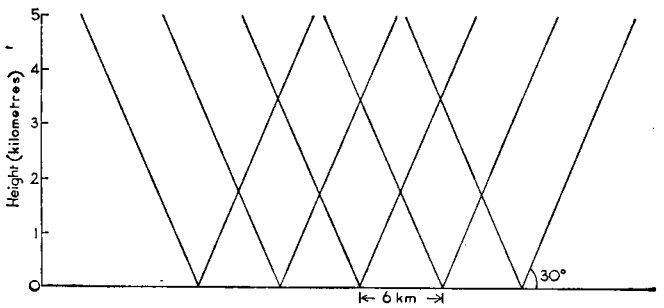

FIGURE 2. Relative positions of cones of observation during a series of 30° rotations repeated every 6 minutes in a pattern moving at 60 km/h.

Computations have been made relative to 600 m in Figure 1 since, because of the small area of observation, the errors become excessive at lower heights. Also because the area covered by the observations at low altitudes is small the divergence may be dominated by small-scale quasi-stationary topographical effects, producing a bias towards either convergence or divergence. Since the observations are over a cone the computed velocity profile would be over-influenced by these low-level local effects. (Ideally the observations should be made over a cylinder, in which case low-level local effects would be compensated for at higher levels to give a velocity more representative of the larger scale.)

(ii) *Aerial pointing vertically.* The accuracy with which vertical air motion can be determined with the aerial pointing vertically has been considered in detail by Caton,[9] especially in Sections 3 to 5 of his paper. The technique will only be summarized here.

Above the melting (i.e. acceleration) layer it is assumed that the smallest particles detected by the radar have terminal velocities between 0·5 and 1·0 m/s. Any echo displayed as rising is considered a definite indication of updraught; echo descending with velocity between 0 and 0·5 m/s is due to (*a*) updraught, or (*b*) echo spreading from adjacent velocity channels or (*c*) small-scale turbulence. Whenever there is a strong signal in any channel, spreading (*b*) occurs because there is not a sharp cut-off at the edges of the filter constituting each velocity channel. Small-scale turbulence (*c*) can usually be identified since it broadens the velocity spectrum without altering the velocity at the spectrum peak. Only when (*b*) and (*c*) are considered unlikely is upward motion assumed. Similarly if there is no echo descending more slowly than 1·0 m/s, a downdraught is indicated. Further indication of a downdraught is given if precipitation above the melting layer falls with a velocity exceeding 3 m/s, since this is greater than the fall-speed of any frozen particles expected in frontal precipitation. It is considered that vertical velocities in excess of about 0·5 m/s were determined in this way with an accuracy of about $\pm 0{\cdot}25$ m/s.

Caton[10] has shown that in widespread rain the minimum detectable terminal velocity is almost always within the interval 1·5 to 2·5 m/s. This is used as an indicator of air motion, following reasoning similar to that in the previous paragraph. Vertical velocities in excess of about 1·0 m/s can be determined but with an accuracy of only about $\pm 0{\cdot}5$ m/s because of the uncertainty in the exact terminal velocity of the smallest detectable raindrops. Downdraughts are also inferred when drops are falling at 10 m/s or more.

2.4. *Isentropic analysis*

Isentropic analyses on the synoptic scale are used to describe the large-scale airflow in frontal regions and to derive, where possible, vertical air motions on this scale. Routine radiosonde data were used. The method of analysis was basically that used by Green *et alii*,[11] who subtracted the motion of the major synoptic feature from the observed winds and plotted these relative winds on maps drawn for constant potential temperature θ. The use of such charts enables vertical velocities to be estimated assuming adiabatic conditions. However, Green *et alii* were considering air movements over periods of several days on the large scale. Since areas of cloud and precipitation covered only a small fraction of the total area of their analysis they considered that the errors arising from non-isentropic flow in such regions were not serious. In the present study interest is primarily in the flow, especially vertical air motion, in these very areas and the wet-bulb potential temperature, θ_w, rather than θ, is considered a more nearly conservative property.

It was found that θ_w surfaces could be drawn with confidence in frontal regions, although in other areas the same value of θ_w sometimes occurred at more than one height, thus occasionally preventing this type of analysis. In the present paper flow over a period of hours rather than days is considered, so that any errors arising from θ_w not being fully conserved should be small. This is especially true in frontal zones, where there is a large gradient of θ_w in the vertical and any small change in the value of θ_w produces only a small vertical displacement compared with the flow assuming constant θ_w. The greatest difficulty in the analysis was found to be in drawing isobars accurately on the θ_w surfaces, the data being so sparse that the orientation of the isobars (which determines the upslope component of the relative flow) was generally no more accurate than $\pm 15°$ in the Pershore area.

2.5. *Form of presentation*

As far as is possible the analysis of each case is presented in a similar format. The results are presented as a series of figures, and features common to the figures in each of the studies will now be considered.

(i) *Synoptic situation.* Surface features, cross-sections and relative-flow θ_w charts have been used to describe the synoptic situation. Charts were generally drawn for a fixed time but when a steady state existed data from other times were included. A steady state was assumed if there was no change in the frontal pattern and the pressure field relative to it, or in the velocity of movement of the pattern, during the period of the observations. On the θ_w surfaces the winds are relative to the movement of the system which was taken as the movement of the frontal zone producing the precipitation. It is considered that these relative winds were generally accurate to about $\pm 15°$ in direction.

(ii) *Horizontal wind field.* A height–time section of the overhead wind field deduced from the Doppler radar (see Section 2.2.) is shown for each occasion. The time-scale is reversed on the figures to facilitate comparison with the synoptic charts, west then being on the left of the section. Winds were estimated every 140 m of height during an aerial rotation and rotations were approximately 5–10 minutes apart. A horizontal distance scale, assuming a steady translation of the pattern over the radar, is shown. The winds at the base of the figures were those recorded by an anemometer 0·5 km east of the radar. Where possible the frontal position is included on the figures; this was deduced from the synoptic data.

(iii) *Divergence field.* Divergence values were calculated whenever there was negligible small-scale air motion (see 2.2.). Calculations were not made in the melting layer (the middle of which is approximately at the 1°C isotherm) because of the rapidly changing fall-speed. The results are presented as height–time sections. The density of observation points on these sections is similar to that for the horizontal wind field and that for Figure 7 of Harrold.[4] The surface rate of rainfall 0·5 km east of the radar is shown at the foot of these figures. Wind-shear data from the radar observations were used to deduce frontal boundaries in this set of figures.

(iv) *Vertical velocity.* Vertical velocity profiles were calculated from the divergence measurements in snow and are expressed relative to the vertical velocity at (*a*) the melting layer or (*b*) the base of the echo if this was above the melting layer, or (*c*) about 600 m (see 2.3.). Errors during rain, especially at an elevation of 30°, were too large to permit the estimation of meaningful velocities. The velocity profiles were generally means over tens of minutes in order to smooth out any short-period irregularities in the divergence pattern (see 2.3.). A height–time section of the vertical velocity deduced from observations with the aerial pointing vertically is also shown for cases when significant motion could be detected in this way.

3. CASE STUDIES

3.1. *Summary of case studies*

Table I summarizes the case studies presented in this paper. The days are grouped so that as far as possible similar synoptic situations are adjacent to each other. Fronts usually approach the British Isles from the west and the cases 9 April 1965, 13 November 1964 and 21 August 1965 are most representative of this type of situation. The other three studies are of less common situations.

TABLE 1. *Summary of case studies*

Date	Type of front over Pershore	Height of 0°C isotherm during precipitation	Surface wind direction
20 Jan. 1965	Warm front or occlusion	Surface	SE
9 Apr. 1965	Warm front	1–2 km	SSW
13 Nov. 1964	Upper warm front	2½ km	SSW
21 Aug. 1965	Warm front	2 km	SSW
29 Nov. 1965	Cold front	Surface	NW
16 June 1965	Warm front or occlusion	2 km	SW–W

3.2. 20 JANUARY 1965

Synoptic situation (Figures 3, 4(*a*) and (*b*))

Both the surface and upper air features moved steadily at 295° 60 km/h with negligible development between 0000 and 0600 GMT, suggesting a steady state. Data for 0000, 0600 and, with some caution in interpretation, 1200 GMT have been included on the relative-flow θ_w charts (Figures 4(*a*) and (*b*)).

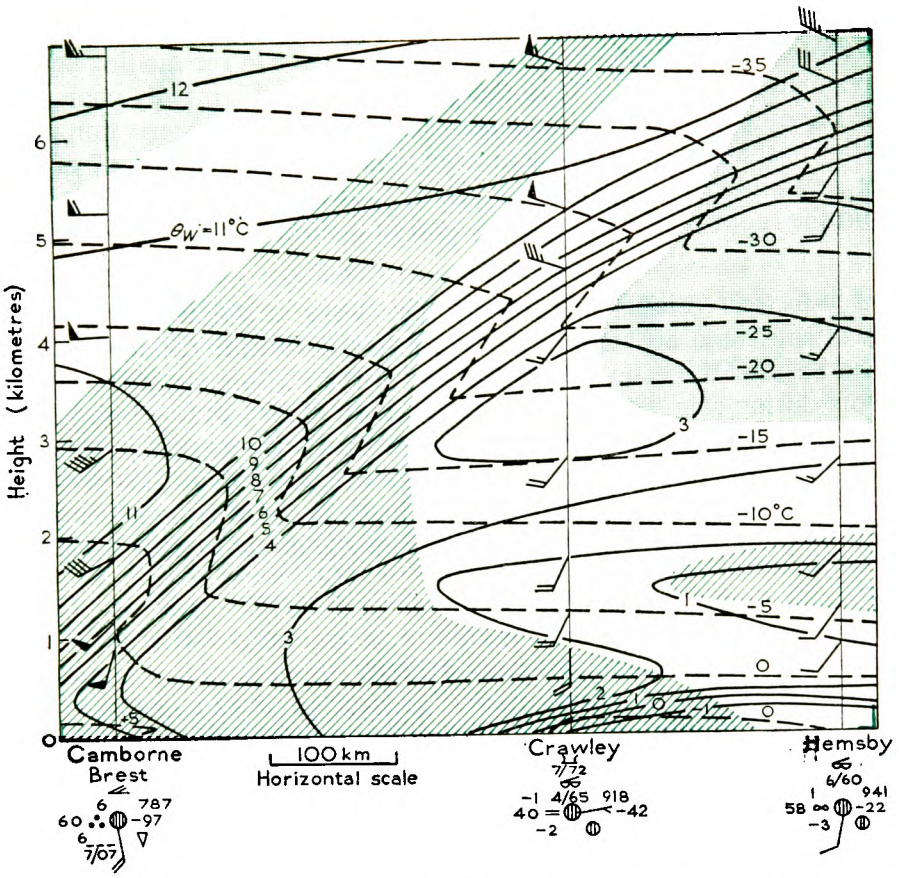

FIGURE 3. 20 January 1965. Cross-section from between Camborne and Brest to Hemsby (along line AB in Figure 4) at 0000 GMT.

——— Wet-bulb potential temperature (°C) — — — Isotherms (°C)

Green diagonally-hatched areas denote dew-point depressions <5 degC; green stippled areas denote depression >10 degC. Actual winds are shown (a full barb represents 5 m/s).

The most marked synoptic feature was the pronounced frontal zone (Figure 3), with a 7 degC change of θ_w in a height of about 1 km. The $\theta_w = 5$°C surface (Figure 4(*a*)), representative of the base of the frontal zone, shows a strong moist south-easterly (relative to the system) flow in the Pershore area. An analysis of both θ_w and θ surfaces at lower levels (not shown) indicates that the flow there was broadly similar to that at $\theta_w = 5$°C. Relative winds were about parallel to the isobars, but because of the large relative wind speeds and the steep slope of the θ_w surface even an angular separation of the relative winds from the isobars which was too small to be discerned in the analysis (because of possible, though small, errors in the orientation of the isobars) would have resulted in appreciable vertical air motion. Consequently it is not possible to reach firm conclusions about even the sign of the low-level vertical air motion from this analysis. On the other hand the wind component up the $\theta_w = 10$°C surface (Figure 4(*b*)) clearly shows that there was an ascending tongue of moist air (dew-point depression <5 degC) over Pershore. The vertical velocity is estimated from Figure 4(*b*) to have been about 2×10^{-2} mb/s. The ascent of this moist air was obviously a

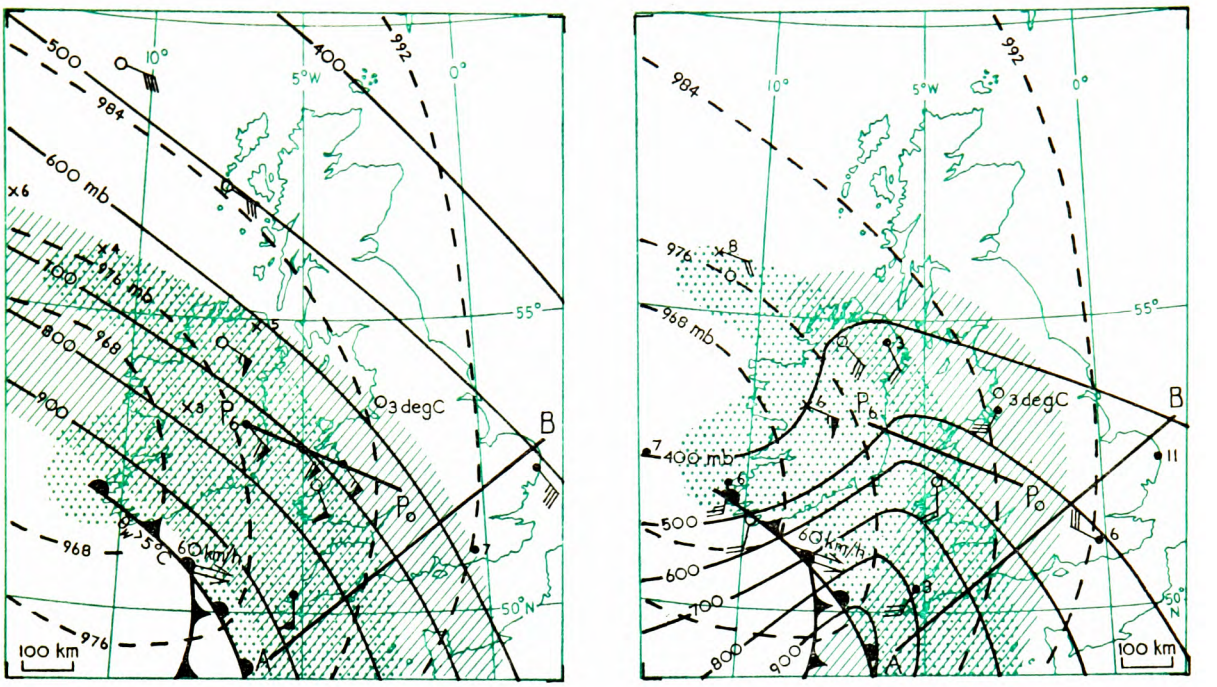

FIGURE 4. 20 January 1965. Relative-flow charts for (*a*) $\theta_w = 5$°C surface and (*b*) $\theta_w = 10$°C surface between 0000 and 1200 GMT.

. 0000 GMT data o 0600 GMT data x 1200 GMT data
——— Isobars on isentropic surface – – – Sea-level isobars at 0000 GMT
P_0———P_6 Position of radar relative to the fronts from 0000 to 0600 GMT
AB Line of cross-section in Figure 3
Surface fronts at 0000 GMT, in usual notation

Data are positioned relative to the depression which, together with the upper air pattern, was moving steadily without development during the period.

Green diagonally-hatched areas denote dew-point depression <5 degC on the isentropic surface (values are plotted to the right of data position); green stippling shows the extent of precipitation at the ground at 0000 GMT. Winds are relative to the movement (295° 60 km/h) of the depression. The position of the British Isles is relative to the system at 0000 GMT.

(*a*) $\theta_w = 5$°C surface

The chart, which is representative of the air flow beneath the front, clearly shows a strong moist south-easterly flow in the Pershore area. This flow is approximately parallel to the isobars on the isentropic surface.

(*b*) $\theta_w = 10$°C surface

The chart, which is representative of the top of the frontal zone, shows moist air ascending over Pershore for most of the period of the radar observations.

contributory cause of the precipitation, but the extension of the surface precipitation west of this high-level moist tongue is evidence that there was also some ascent of the moist air at lower levels. Over central and east England evaporation in the dry air beneath the frontal zone prevented precipitation reaching the ground.

At Pershore the precipitation was mostly of wet snow at the surface. It began at 0200 GMT, although there was radar echo aloft before this which reached the ground some miles west of the radar, and continued for 12 hours. Radar observations were made until 0600 GMT, being terminated when thick slush on the radar radome produced severe attenuation.

Horizontal wind field (Figure 5)

Figure 5 shows a veering of wind with height, especially in the frontal zone and a backing with time below 2 km. There was a speed minimum at 4 km and a maximum at 1 km. Radiosonde winds for 900 m (not shown) indicated that at this level a wind maximum was over Pershore at 0600 GMT so the low-level wind field in Figure 5 can be considered as a section through the eastern (right-hand side) of a jet (but the section is not normal to the wind). Note also that the highest echo compares well in time with the passage of the axis of the upper moist tongue (Figure 4 (*b*)) over Pershore. There was a distinct backing of the wind with time above about 3 km (about 20° at 4 km) during the passage of the highest echo; a detailed

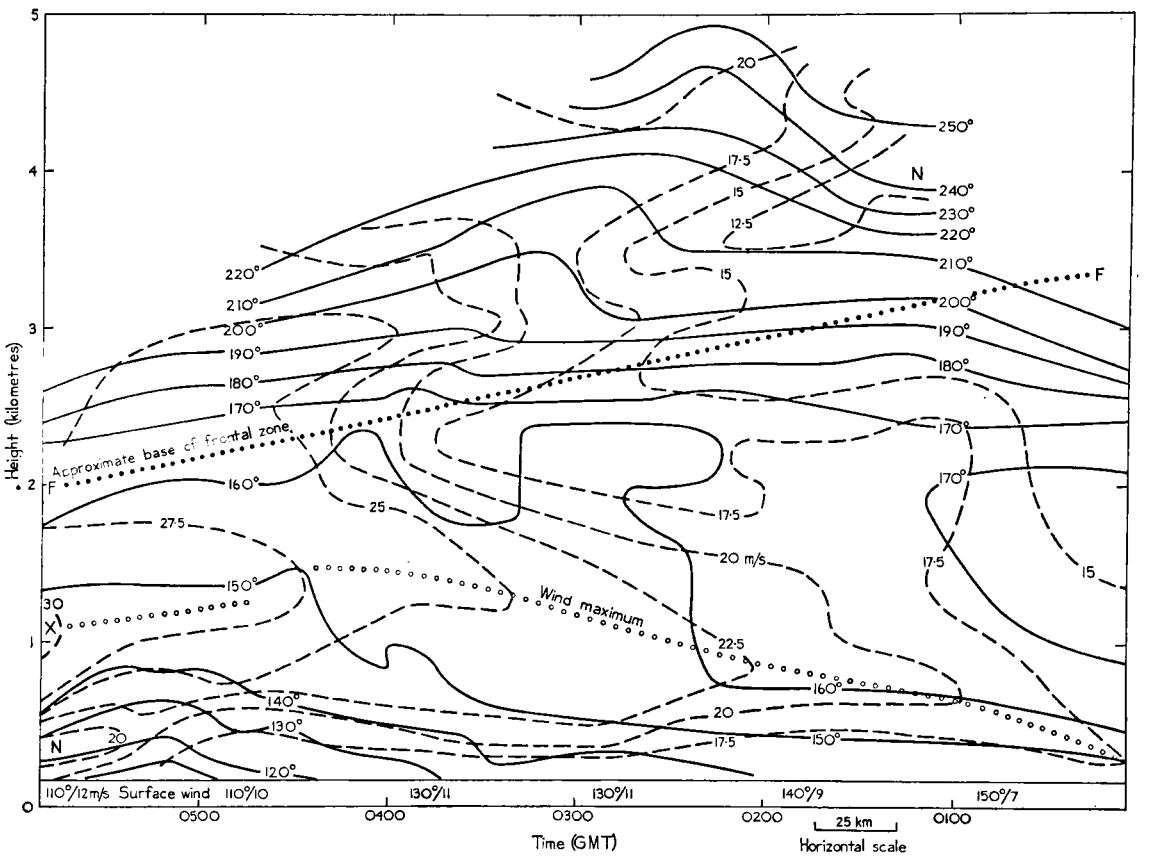

FIGURE 5. 20 January 1965. Height–time section of wind field over Pershore.

——— Direction isopleths - - - Speed isopleths

X Denotes speed maximum N Denotes speed minimum

F . . . . F Base of frontal zone, deduced from synoptic data

The horizontal scale is based on the assumption that the depression was moving at 60 km/h. Pershore surface winds are shown at the foot of the diagram.

analysis of 600 and 500 mb levels showed no evidence of this wind fluctuation, but because of the spacing of the radiosonde observations, even when incorporating those at different times, it is not possible to state categorically that this mesoscale feature was not a manifestation of a synoptic-scale feature extending over some hundreds of kilometres.

Divergence field (Figure 6)

The limited data shortly after midnight show divergence at about 2 km height. The range height indicator (RHI) radar at Pershore showed that the echo at this level was part of a large fallstreak which was being generated to the south, so the existence of the divergence, implying downdraught, was not incompatible with the presence of the precipitation as the volume

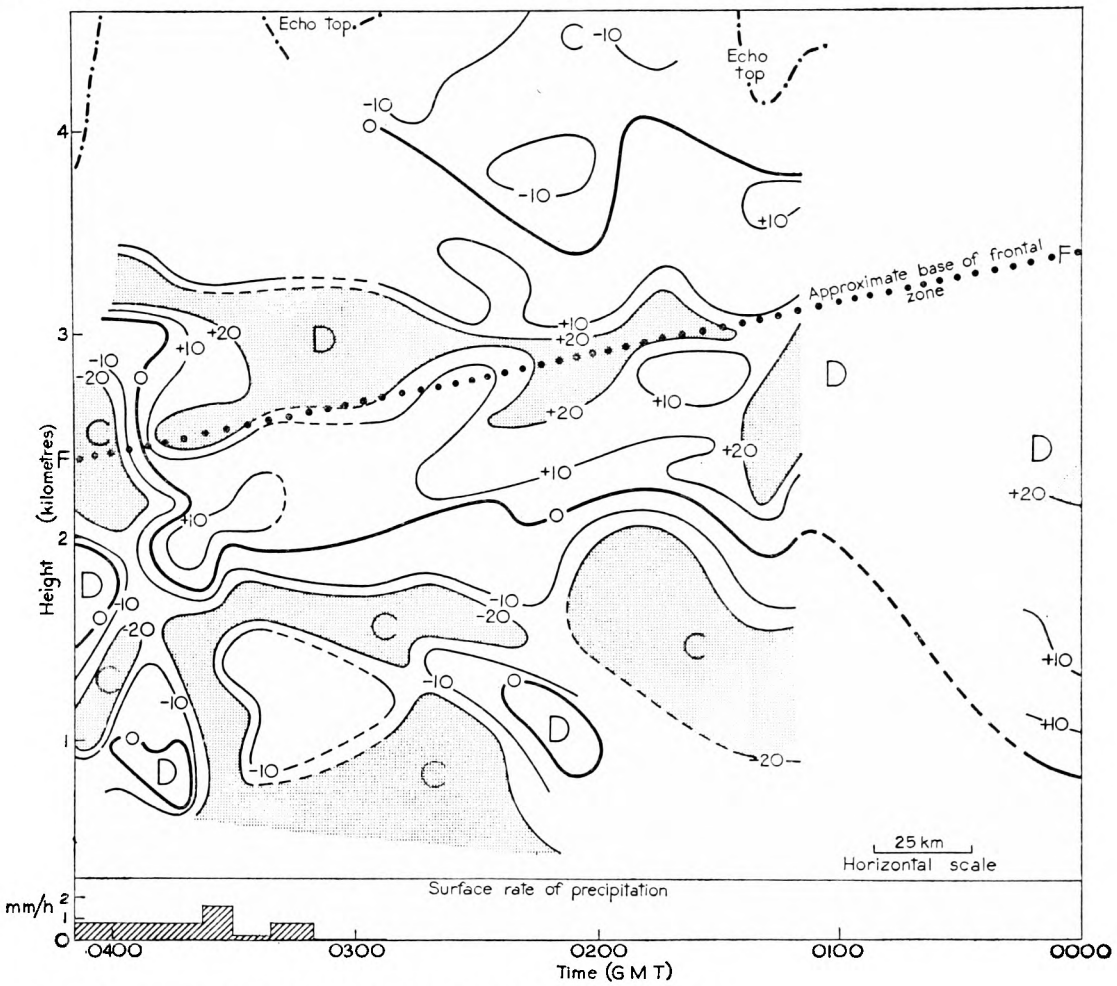

FIGURE 6. 20 January 1965. Height–time distribution of divergence.

C Denotes convergence D Denotes divergence

– · – · Echo top

F . . . . F Base of frontal zone, deduced from synoptic data and from wind shears shown in Figure 5

Regions of $|D| > 20 \times 10^{-5}$/s are shaded

Measurements were taken in snow throughout, and during a period when there were negligible fluctuations in the precipitation fall-speed.

scanned by the Doppler was outside the generating area. For most of Figure 6 there are only small changes in the pattern. A layer of divergence, which was at about the level of the base of the frontal inversion, was sandwiched between two layers in which convergence predominated. After 0340 the pattern underwent marked changes and variable vertical air motion became established, preventing further accurate divergence measurements after 0410.

Vertical air motion (Figures 7, 8)

Between 0200 GMT, when precipitation first reached the ground, and 0400 GMT the maximum velocity (Figure 7) was about $3{\cdot}5 \times 10^{-2}$ mb/s, relative to that at about 400 m. The trend of the lower portions of the two profiles suggests that the vertical velocity at 400 m was about 10^{-2} mb/s. After 0330 the vertical velocity was large enough to be estimated with the aerial pointing vertically (Figure 8). Note that Figure 8 overlaps in time the second profile of Figure 7. There was general agreement below 3 km (the maximum height of the second profile) with upward motion of the order of 0·5 m/s (5×10^{-2} mb/s). After 0415 a layer of downdraught was also identifiable.

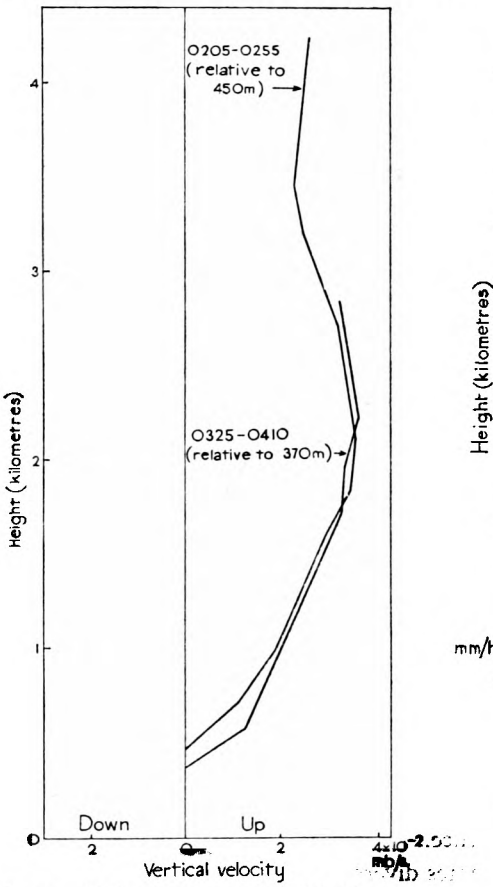

FIGURE 7. 20 January 1965. Vertical velocities deduced from Figure 6.

Data are meaned over the periods 0205–0255 and 0325–0410 GMT, and the velocities are relative to those at 450 m and 370 m respectively. (10^{-2} mb/s ≃ 10 cm/s)

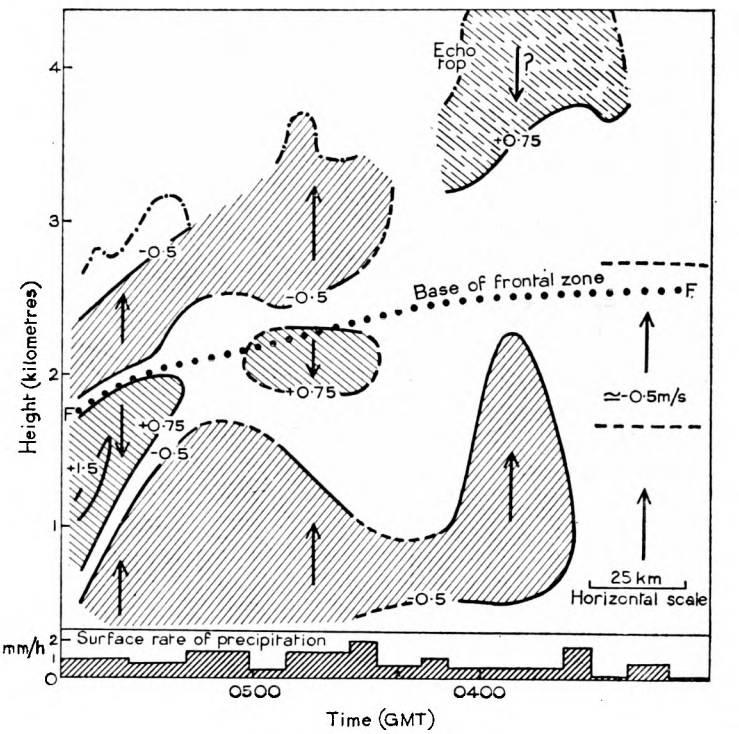

FIGURE 8. 20 January 1965. Height–time section of vertical velocity deduced from measurements taken with the radar aerial vertical.

F . . . . F Base of frontal zone, deduced from Figure 9

Regions of identifiable vertical air motion >0·5 m/s upwards and >0·75 m/s downwards are shaded, and arrows indicate the direction of motion.

The pecked lines before 0330 GMT are extracted directly from Figure 7 and are boundaries of upward vertical air motion of approximately 0·5 m/s.

There was no connexion between the height of the echo top and the rate of rainfall (base of Figure 6 or 8), even when allowance was made for the one hour it took the snow to fall from 4 km; in fact the rainfall increased as the echo top lowered. There was a broad correlation of rainfall rate with vertical velocity, the rainfall rate increasing as the two layers of

ascent greater than 0·5 m/s became established. It is not to be expected that rainfall variations over tens of minutes could be correlated in detail with the vertical velocities in Figure 8, since the precipitation at the ground fell from streamers originating out of the plane of the height–time section.

Discussion of 20 *January* 1965

Vertical and horizontal air motions (Figures 5, 7 and 8) have been combined to obtain the three-dimensional flow relative to the front (Figure 9). The figure was drawn assuming that the height–time sections were representative of spatial conditions. These trajectories only show airflow in the plane of the section, corresponding to a vertical section along P_0P_6 in Figures 4(*a*) and (*b*). Below about 2 km, relative winds were in fact parallel to this section but at higher levels there was an increasing flow into the plane of the section. The most

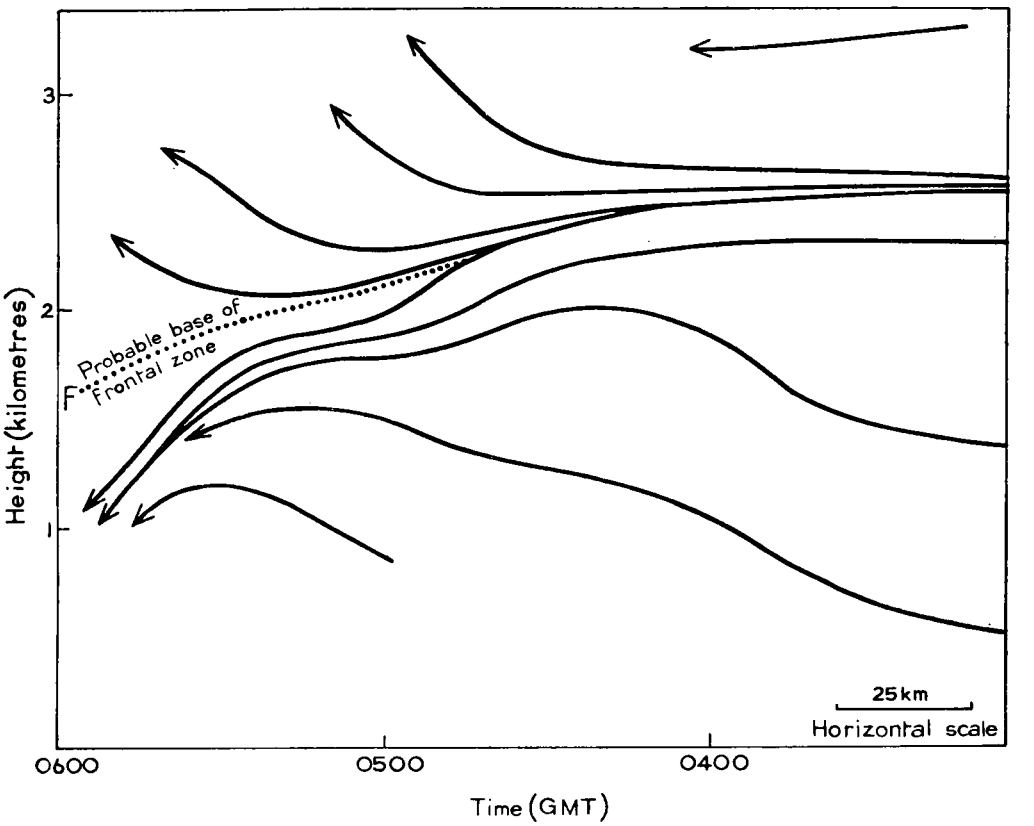

FIGURE 9. 20 January 1965. Trajectories of airflow relative to the movement of the depression, derived from Figures 5 and 8.

Spatially the section is orientated along the line P_0——P_6 in Figure 4. Beneath the front the relative flow is parallel to this line so that the trajectories approximate to the three-dimensional relative flow, but within the frontal zone there is some motion into the plane of the paper.

striking feature of Figure 9 is the stream of descending air at the western end of the section. The base of the frontal zone at 0300 GMT was at about 2½ km and this appeared to mark the dividing line between ascending and descending air in Figure 9.

It is instructive to compare the radar-derived vertical velocities with the relative-flow θ_w analysis. Above 4 km at around 0230 the radar-computed vertical velocity was about

$(4 \pm 1{\cdot}25) \times 10^{-2}$ mb/s (relative to the ground), averaged over a 50-minute period (about 50 km in space). The θ_w analysis on the other hand indicated 2×10^{-2} mb/s at 4·8 km (Figure 4(*b*)). It appears that the θ_w analysis, although giving the order of magnitude, underestimated the rate of ascent. The radar showed similar velocities at lower altitudes, although a persistent layer of downdraught also became established later; the θ_w analysis, because of the difficulty of determining the exact orientation of the isobars (see 2.4.), did not reveal these features. It appears that on this occasion the θ_w analysis, although clearly displaying the large-scale airflow, only provided a limited amount of information as to the vertical velocities that occurred in the region of precipitation, probably because the amount of data was insufficient for an accurate mesoscale analysis.

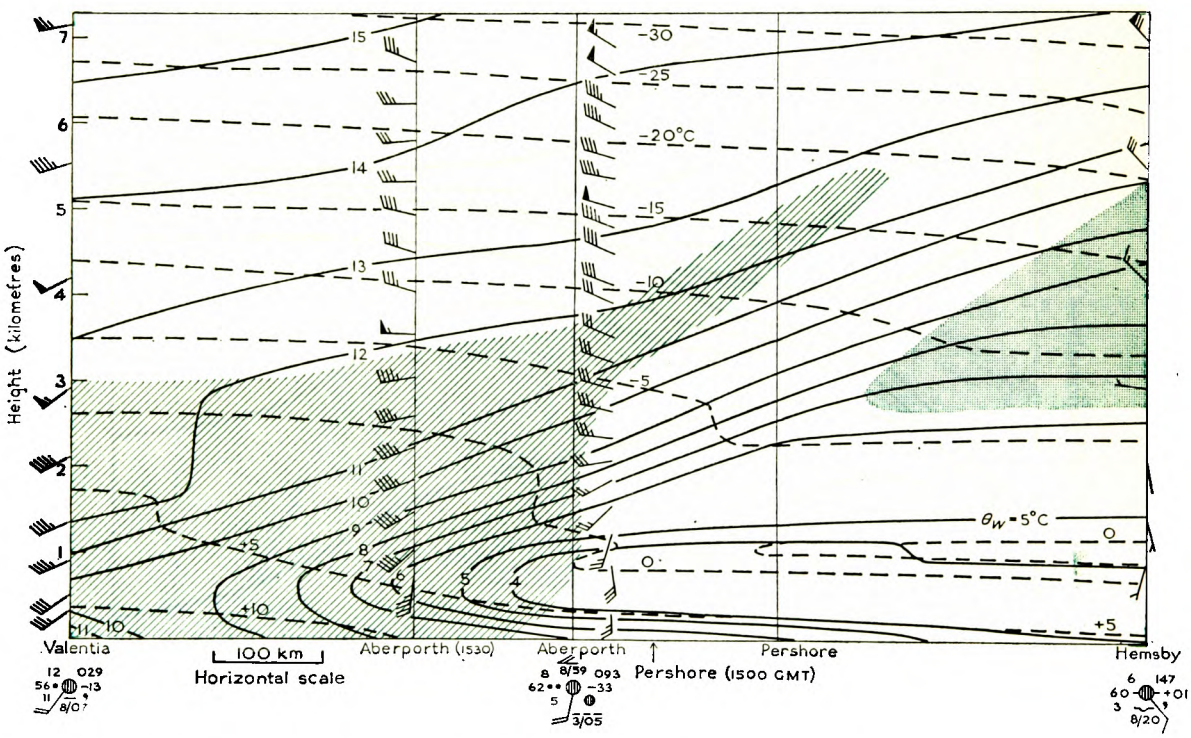

FIGURE 10. 9 April 1965. Cross-section from Valentia to Hemsby at 1200 GMT.

——— Wet-bulb potential temperature (°C) — — — Isotherms (°C)

Green diagonally-hatched area denotes dew-point depression <3 degC; green stippled area denotes depression >10 degC. Actual winds are shown.

3.3. 9 APRIL 1965

Synoptic situation (Figures 10, 11(*a*) and (*b*))

The rain on this occasion was associated with a warm frontal zone moving at 240° 45 km/h and this case is representative of a common frontal situation in the British Isles. The axis of the heaviest rain, excluding orographic effects, was about 170 km ahead of the surface front

(Figure 11). There was also a subsidence inversion at a height of about 1 km ahead of the front (Figure 10). The θ_w charts (Figures 11(*a*) and (*b*)) show that the relative flow was generally light and, within the accuracy of the analysis, along the isobars, indicating that any vertical air motion was small. The only reasonably firm indication of ascent in the Pershore area was near 1800 GMT, and even then it was only about 3×10^{-3} mb/s. At Pershore, continuous rain lasted from 1500 to 1815, but its intensity was less than 2 mm/h except for a short time around 1740. Radar observations were made throughout the period of rain.

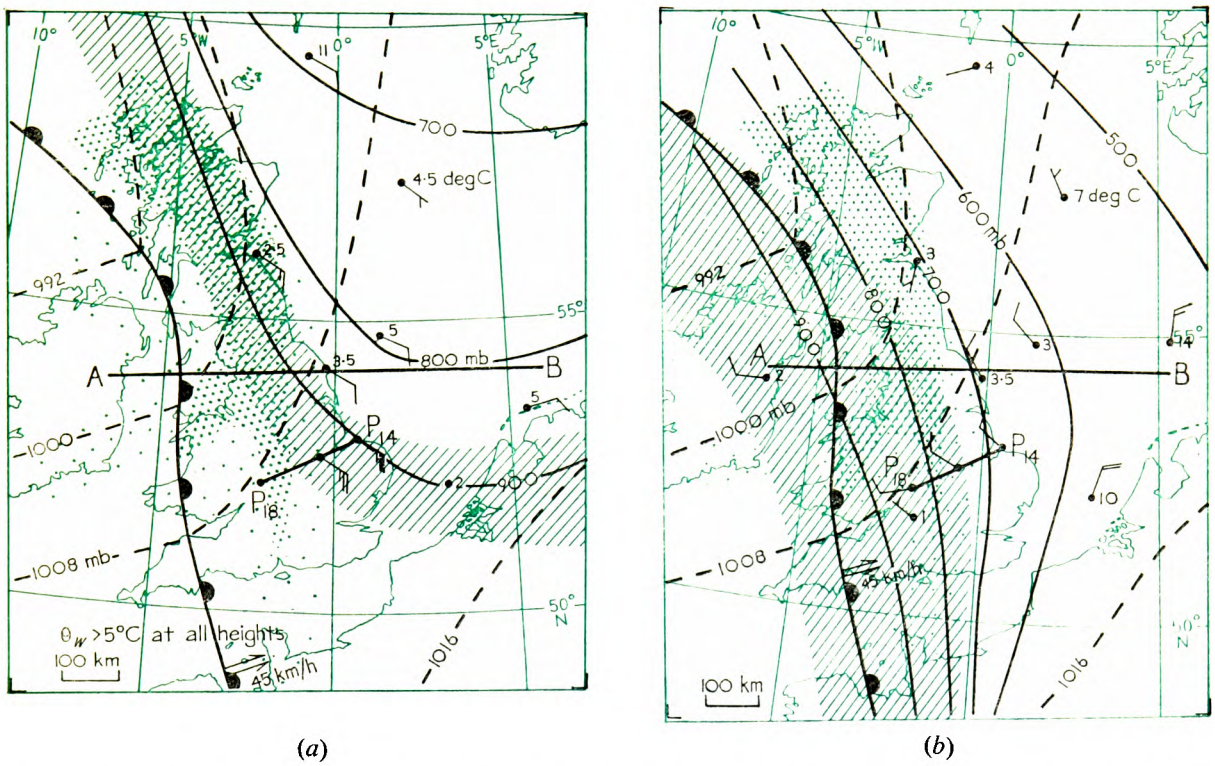

FIGURE 11. 9 April 1965. Relative-flow charts for (*a*) $\theta_w = 5°C$ surface and (*b*) $\theta_w = 10°C$ surface between 1200 and 1800 GMT.

. 1200 GMT data (displaced relative to front)
——— Isobars on isentropic surface - - - Sea-level isobars at 1800 GMT
P_{14}———P_{18} Position of radar relative to the fronts from 1400 to 1800 GMT
AB Relative position at 1800 of line of cross-section in Figure 10
Surface fronts at 1800 GMT, in usual notation

Green diagonally-hatched areas denote dew-point depression <3 degC on the isentropic surface (values are plotted to the right of data position). Heavy green stippling shows the extent of continuous moderate or heavy rain at the ground, light stippling the extent of slight rain. Winds are relative to the movement (240° 45 km/h) of the warm front.

(*a*) $\theta_w = 5°C$ surface

The chart, which is representative of the air flow beneath the front, shows a moist but rather weak south-easterly flow in the Pershore area.

(*b*) $\theta_w = 10°C$ surface

The chart, which is representative of the airflow above the front, also shows a weak flow, with any ascent $<10^{-2}$ mb/s.

Horizontal wind field (Figure 12)

There was a pronounced wind shear across the frontal zone. At 1430 near 1¾ km the thermal wind was 12 m/s over a height layer of 350 m, and if the air was in geostrophic balance this implies a horizontal temperature gradient of about 1 degC in 10 km. There was a slight tendency for the lowering of this shear zone to take place in steps, these beginning at about 1450, 1620 and 1720. It is not possible to determine whether this effect was local to Pershore, or whether it represented the passage of discontinuities ('steps') in the frontal zone.

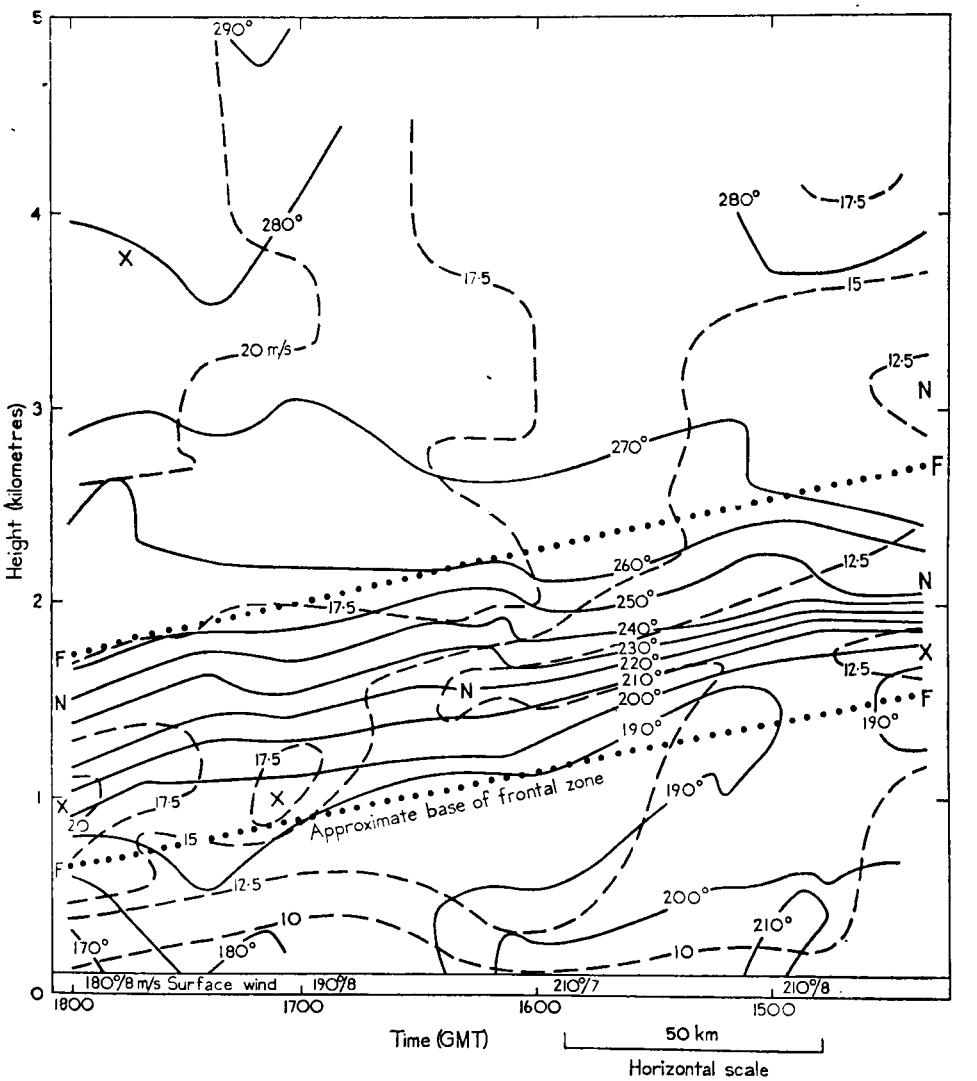

FIGURE 12. 9 April 1965. Height–time section of wind field over Pershore.

——— Direction isopleths - - - Speed isopleths
X Denotes speed maximum N Denotes speed minimum
F . . . . F Boundaries of frontal zone, deduced from synoptic data

The horizontal scale is based on the assumption that the warm front was moving at 45 km/h. Pershore surface winds are shown at the foot of the diagram.

Divergence field (Figure 13)

The distribution of divergence was very patchy, with no persistent pattern, although spatially, divergence predominated over convergence. Many of the individual estimates of divergence were significant (exceeding twice the probable error) and it is thought that the observed patchiness was a real feature and not the result of errors in the observations.

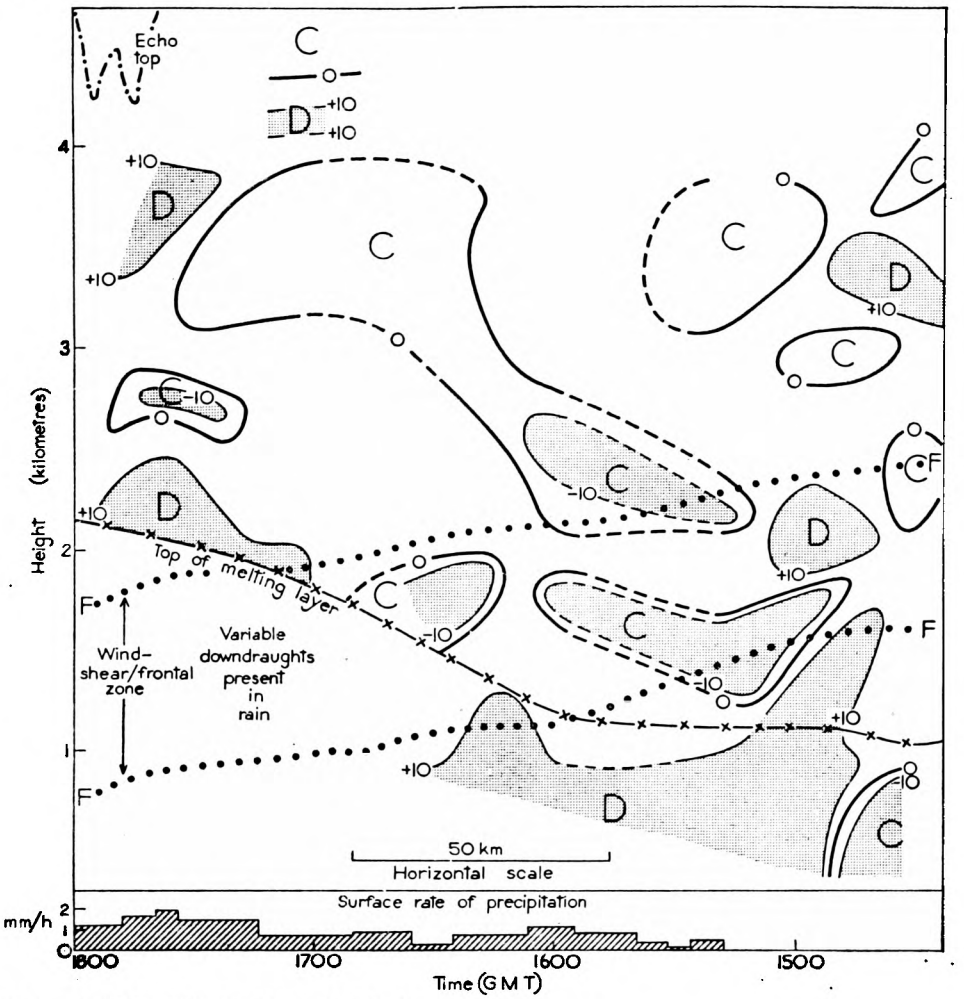

FIGURE 13. 9 April 1965. Height–time distribution of divergence.

C Denotes convergence D Denotes divergence

– · – · Echo top

F . . . . F Boundaries of frontal zone, deduced from synoptic data and from wind shears shown in Figure 12

Regions of $|D| > 10 \times 10^{-5}$/s are shaded

Isolated values of $|D| > 20 \times 10^{-5}$/s were recorded but were too localized to enable contours to be shown. Measurements were not possible below 2 km after 1700 GMT because of variable air motion. The echo top overhead was above 4·5 km except for a short period towards the end of the observations.

Vertical air motion (Figure 14)

The vertical velocity profiles are means over periods ranging from 6 minutes to 20 minutes, depending on the steadiness in time of the divergence pattern, and the velocities are all

relative to that at the top of the melting layer. The trend of the lower portions of the profiles, together with the persistent divergence in the rain, indicates the possibility of a downward velocity at that level. The velocities on Figure 14 are small (generally about $0{\cdot}5 \times 10^{-2}$ mb/s) and many are of the same order of magnitude as the probable error (see Figure 1). It appears that upward motion was confined to only short periods.

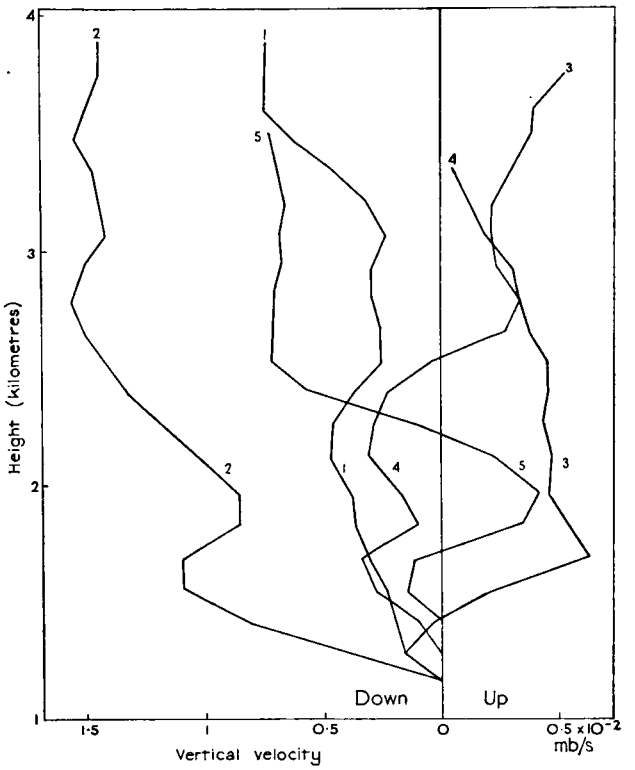

FIGURE 14. 9 April 1965. Vertical velocities deduced from Figure 13.

Data are meaned over the periods (1) 1424–38, (2) 1443–1503, (3) 1510–16, (4) 1600–06, (5) 1614–20 GMT, and the velocities are relative to those at the top of the melting layer. Note the small magnitude of these velocities compared with the other case studies.

The analysis of the observations made with the radar pointing vertically indicated no air motion exceeding 0·25 m/s in snow. However, between 1702 and 1800 there was downward motion in the rain and this exceeded 2 m/s occasionally. The heaviest rate of rainfall occurred at this time.

Discussion of 9 *April* 1965

Measurements were made during the passage of a synoptically typical warm front. The smallness of the vertical velocity is in at least qualitative agreement with that deduced from the relative-flow isentropic charts. These showed a maximum ascent of about 3×10^{-3} mb/s.

The heaviest rate of rainfall was 2 mm/h at about 1740. At this time there was a persistent downdraught beneath the melting layer and the preponderance of divergence above this layer suggests that some downward motion, although too small to be shown by the observations made with the radar pointing vertically, extended to a height of 4 km. This implies negligible

precipitation growth below this level and above 4 km there was apparently insufficient moisture and ascent (Figure 10) to produce a rate of rainfall of 2 mm/h in a column of the atmosphere. (In a saturated atmosphere a 200-mb layer above 4 km would have to ascend at 0·33 m/s to produce 2 mm/h, assuming 100 per cent efficiency in precipitating.) The reason for this rate of rainfall is not, then, obvious. A possibility is that there was considerable precipitation growth within and close to the melting layer. That there is frequently accretion and/or aggregation close to this layer has been shown by many authors (e.g. Battan[12]) when comparing echo intensities beneath and above the bright band. Another possible explanation is that the precipitation formed in a small generating area that did not pass through the cone of radar observations, although this seems unlikely since the rainfall maximum appeared to be a large-scale feature, extending north–south over several hundred km (Figures 11(*a*) and (*b*)). A third possibility is that the downdraught, although persistent in time, was a very localized feature confined to the Pershore area.

The geographical distribution of rainfall between 0900 and 2100 GMT is shown in Figure 15. There was heavy orographic rainfall on the windward side of mountainous areas. There was also a small area of minimum rainfall (centred on R in the figure) to the lee of the Welsh mountains, but its extent was masked by the general decrease in rainfall southward and

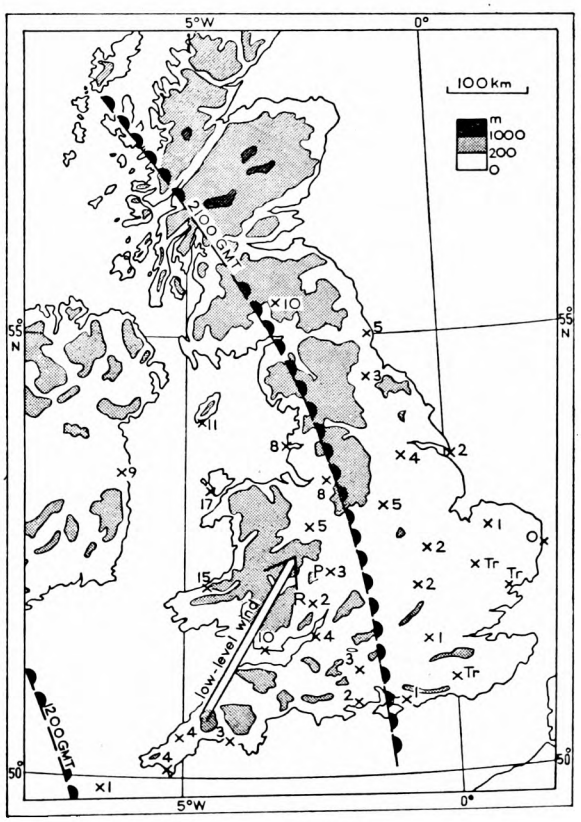

FIGURE 15. 9 April 1965. Rainfall totals (millimetres) 0900–2100 GMT.

P Pershore R Ross-on-Wye

Note the heavy orographic rainfall along the Welsh coast and the rain shadow centred on Ross-on-Wye. The rainfall totals over eastern England are small partly because of the whole of the rain area had not crossed the region by 2100. The arrow indicates the direction of the low-level (900 mb) wind.

eastward. It seems probable, then, that the Doppler observations are representative, at most, of the area to the lee of the Welsh mountains, since the variations shown in Figure 15 are too large to be the result solely of a change in water content of the air without changes in the vertical velocities as well.

3.4. 13 NOVEMBER 1964

Synoptic situation (Figures 16, 17)

Continuous light rain fell at Pershore from mid-morning until about 1600 GMT. Radar measurements were made during the latter part of this period, when Pershore was within the surface warm sector (Figure 17). The cause of this precipitation is not apparent on the surface chart, although it ceased at the passage of a pressure discontinuity as this moved across the country, but the cross-section (Figure 16) shows an upper warm frontal zone over England and Wales and the relative-flow chart (Figure 17) indicates a flow of moist air up this surface. Therefore this feature was one cause of the precipitation. Figure 17 implies a vertical velocity of about 3×10^{-3} mb/s in the Pershore area. However, there was some development of the pattern taking place at this time so that a steady state cannot be assumed and there

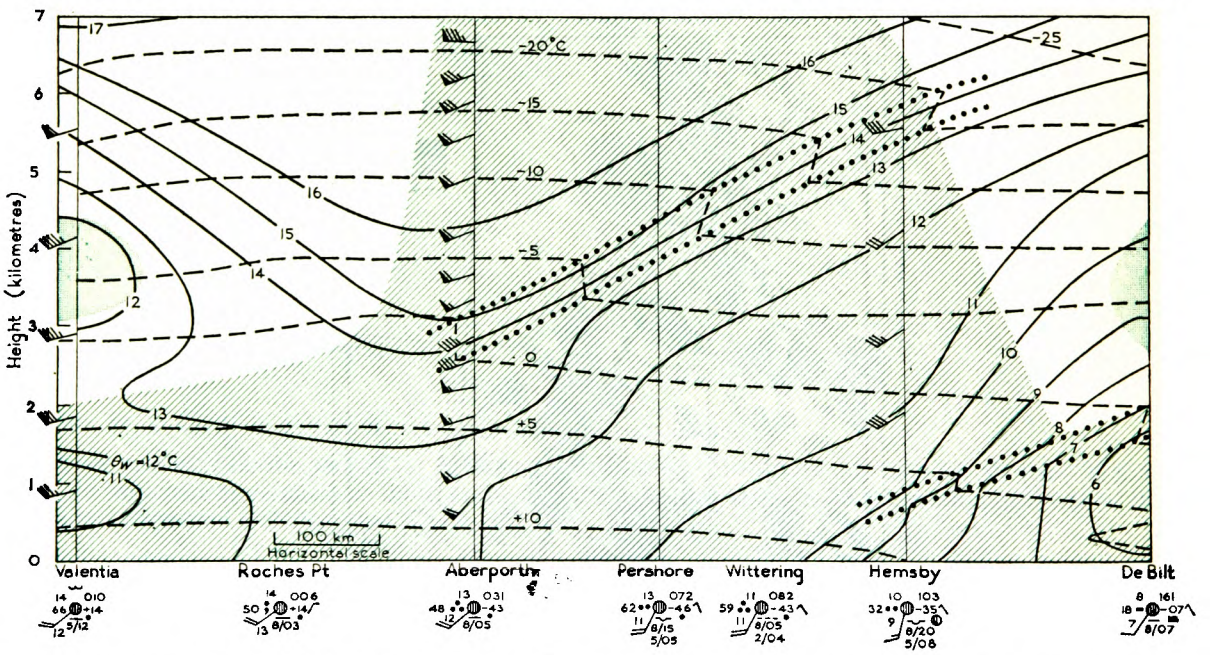

FIGURE 16. 13 November 1964. Cross-section from Valentia to De Bilt (along line AB in Figure 17) at 1200 GMT.

——— Wet-bulb potential temperature (°C) – – – Isotherms (°C)

Green diagonally-hatched area denotes dew-point depression <5 degC; green stippled areas denote depression >20 degC. The double dotted lines emphasize temperature fronts. Actual winds are shown.

was some doubt as to the speed of movement of the precipitation system, leading to uncertainties in the relative airflow; hence the stated vertical velocity is only an approximate value. Relative-flow analyses (not shown) beneath the upper front indicate ascent of approximately 10^{-3} mb/s.

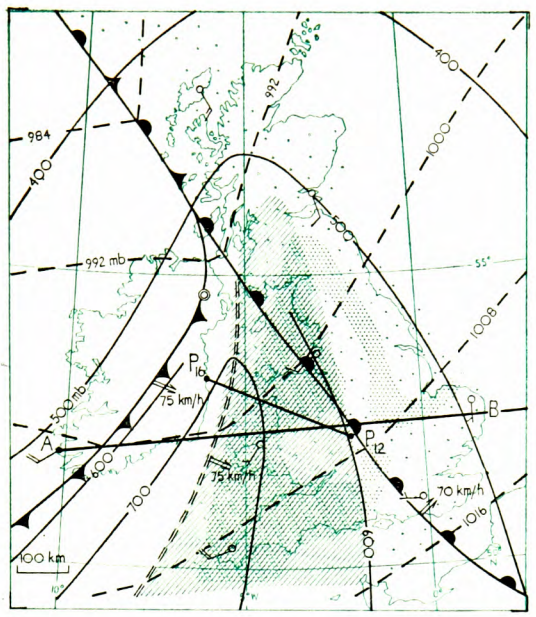

FIGURE 17. 13 November 1964. Relative-flow chart for θ_w = 14°C surface at 1200 GMT.

o 1200 GMT data

——— Isobars on isentropic surface - - - Sea-level isobars at 1200 GMT

P_{12}———P_{16} Position of radar relative to the fronts from 1200 to 1600 GMT

AB Part of line of cross-section in Figure 16

Surface fronts at 1200 GMT, in usual notation

Green diagonally-hatched area denotes dew-point depression <2·5 degC on isentropic surface. Heavy green stippling shows the extent of continuous moderate or heavy rain at the ground, light stippling the extent of continuous slight rain. Intermittent slight rain and drizzle were widespread outside the stippled area. Note that the continuous rain ceases at a marked surface pressure discontinuity which is shown by a double dashed line. Winds are relative to the movement (280° 75 km/h) of the discontinuity. There is some uncertainty in the relative winds because it is not certain that the isentropic surface was moving precisely at the speed of the discontinuity, but ascent seems very probable up the frontal slope.

The 600-mb isobar is not drawn over northern Ireland because of some instability at that level (θ_w decreasing with height).

Horizontal wind field (Figure 18)

The position of the frontal zone on the height–time section was deduced by comparing the winds with those in the cross-section (Figure 16). The winds at Pershore at 1500 GMT were in fact very similar to those at Aberporth at 1200 GMT, so it is assumed that the frontal positions also correspond. The strongest wind shear in the section occurred beneath the front at a height of 1 km. There was little change in wind direction across the front, although a speed minimum is apparent within the frontal zone.

Divergence field (Figure 19)

The melting layer was between 2½ and 3 km so that most of the data were obtained in rain, where the probable errors are greater than in snow. However, many values were significant (exceeding twice the probable error) and the isopleths are considered reliable down to below

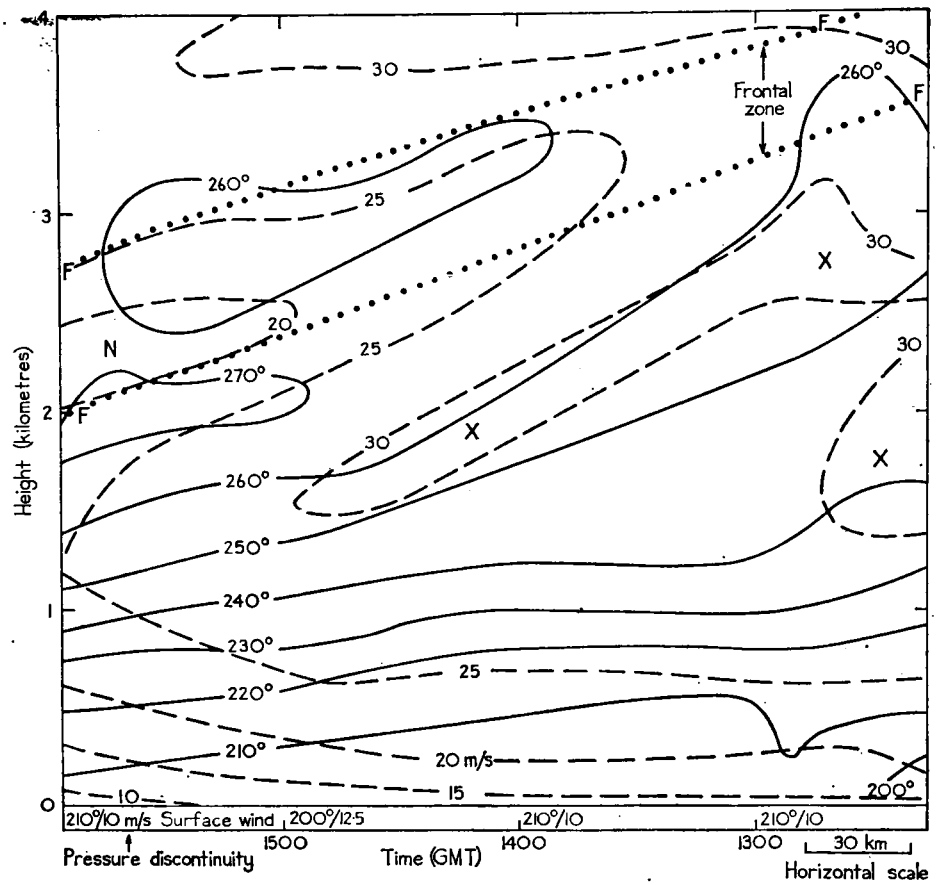

FIGURE 18. 13 November 1964. Height–time section of wind field over Pershore.

——— Direction isopleths - - - Speed isopleths
X Denotes speed maximum N Denotes speed minimum
F . . . . F Boundaries of frontal zone, deduced from synoptic data

The horizontal scale is based on the assumption that the pressure discontinuity was moving at 75 km/h. Pershore surface winds are shown at the foot of the diagram.

1 km. Below about 800 m there was little consistency in the results. Divergence predominated below 2 km and this may be the reason why the upper frontal zone did not extend below this level (Figure 16), i.e. the frontolysis effect of the divergence diminished the horizontal temperature gradient. The change to divergence at 3 km at about 1530 was followed by the disappearance of echo at that level a few minutes later and the cessation of rain at the ground at 1545 GMT, suggesting that the rainfall was determined solely by events at or above this level.

Vertical air motion

Most of the data were obtained in rain, so there was probably a large error in velocities calculated from the divergence and profiles are not shown. Nevertheless, it is possible to make some deductions. Thus, if we approximate the divergent layer to a 1·4 km-deep layer of $D = 20 \times 10^{-5}$/s the downward velocity at 2·2 km would be $2{\cdot}8 \times 10^{-2}$ mb/s relative to that at 800 m. The convergence between 2·2 km and the frontal zone was insufficient to compensate

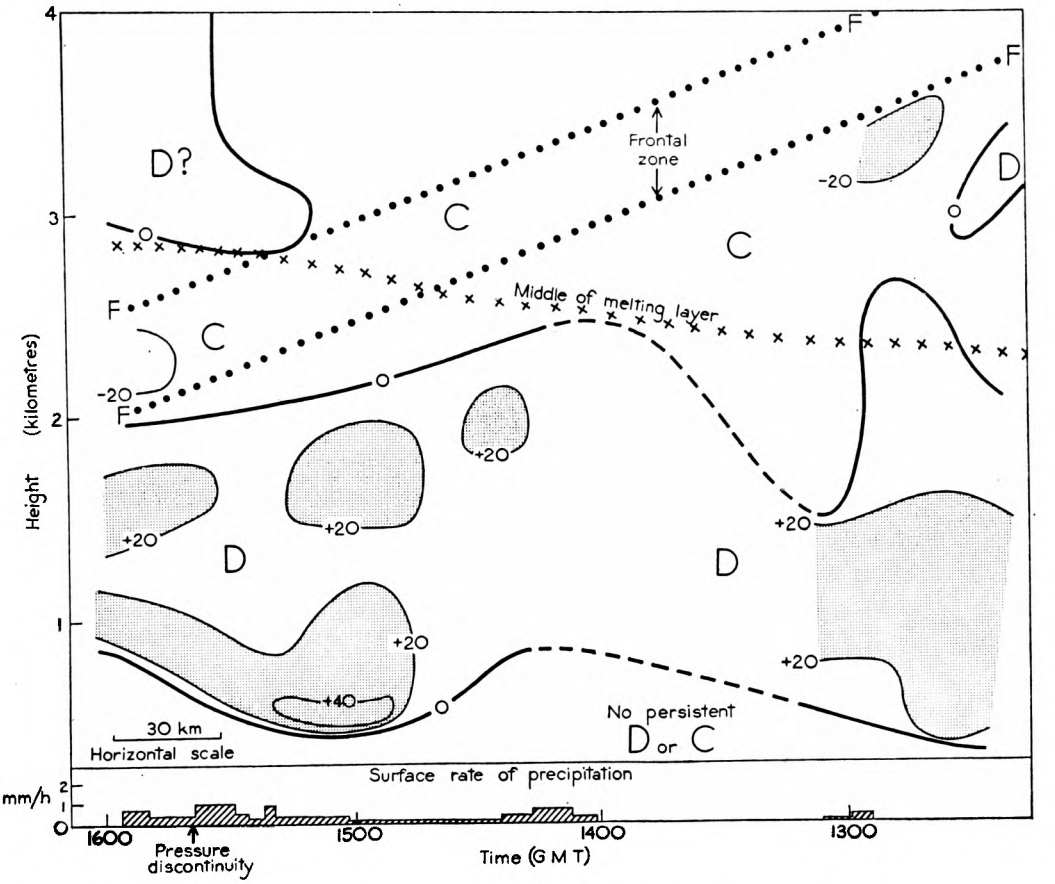

FIGURE 19. 13 November 1964. Height–time distribution of divergence.

C Denotes convergence D Denotes divergence
F . . . . F Boundaries of frontal zone, deduced from synoptic data
Regions of $|D| > 20 \times 10^{-5}$/s are shaded

for all of this divergence and it can be concluded that beneath the frontal zone there was descent of about $(2{\cdot}5 \pm 0{\cdot}5) \times 10^{-2}$ mb/s relative to the velocity at 800 m. Ascent of this magnitude at 800 m would entail convergence of 25×10^{-5}/s below this level; there were no indications of persistent convergence of this magnitude so air beneath the front was descending.

The observations made with the Doppler pointing vertically revealed very little vertical air motion, possibly partly because this technique is less sensitive in rain. There was a short-lived updraught of 0·5 m/s near 3 km at 1250 and very occasional downdraughts were just resolvable between 1·6 and 2·2 km. Conditions seemed turbulent below about 800 m, with short periods of both updraught and downdraught, with a slight preponderance of upward motion.

Discussion of 13 *November* 1964

Radar measurements were made during a four-hour period within a surface warm sector. During this time an upper warm front moved across the area. The following four features show that ascent of moist air up this surface was the sole cause of the rain at Pershore.

(i) Descent beneath the frontal zone. (It was not possible from the radar observations to deduce the air motion at higher levels because of the lack of echo.)

(ii) The rain ceased as the western edge of the front passed.

(iii) A vertically pointing 8-mm radar, which is considerably more sensitive than the Doppler radar in detecting small particles, showed echo to over 8 km. There was a generally regular increase of (range-corrected) intensity down to about 4 km, indicating growth, but no further increase was detectable below this height (except at the melting layer). That is, precipitation growth appeared to be confined to levels above the frontal zone, excluding any effects within the melting layer.

(iv) The rate of rainfall can be computed from a knowledge of the vertical velocity and water content of the air, assuming that all of the condensed water is immediately precipitated and none is stored as cloud (see for example Petterssen[13]). The relative-flow θ_w

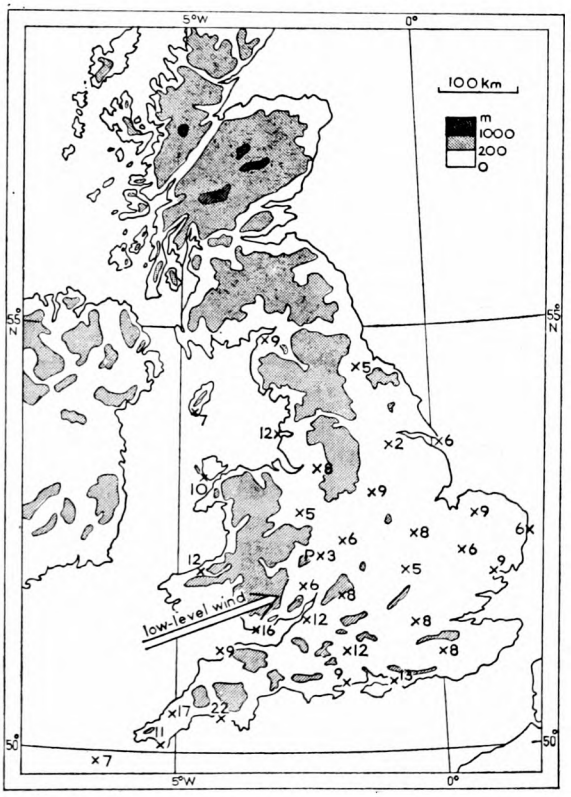

FIGURE 20. 13 November 1964. Rainfall totals (millimetres) 0900–2100 GMT.
P Pershore
Note the rainfall minimum at Pershore. The arrow indicates the direction of the low-level (850 mb) wind.

analysis (Figure 17) indicates ascent of about 5 cm/s at 600 mb, and if this figure was representative of the motion between 600 and 300 mb, the rate of rainfall from this layer would be about 0·37 mm/h. This is almost the same as the mean observed rainfall of 0·4 mm/h over the four-hour period. Thus the synoptic data indicate that the rainfall can be accounted for entirely by ascent above the frontal zone, if none of the condensed vapour is stored aloft.

The relative-flow θ_w chart (not shown) beneath the frontal zone indicates ascent, in conflict with what was observed. It is suspected that this ascent, if real on the synoptic scale, was masked on the mesoscale by the effects of topography. The rainfall totals (Figure 20) for the period 0900–2100 GMT show a pronounced rain-shadow effect, in keeping with the observed downward motion, Pershore being one of the driest places in the country. It seems possible that the divergence maximum below about 1·3 km (Figure 19) was induced by topography, although the maximum around 1·8 km seems to have been at least partly representative of the synoptic scale since it marks the base of the frontal zone.

The Scilly Isles were probably unaffected by topography in this situation. Comparing the rainfall there with quantities measured elsewhere it seems that the effect of the Welsh mountains was approximately to double the amount on the windward side (Figure 20) and to halve it on the lee.

3.5. 21 AUGUST 1965

Synoptic situation (Figures 21, 22 (*a*) and (*b*))

Rain during the early hours of 21 August was apparently associated with a warm front (Figure 22) but the cross-section (Figure 21) shows a complex frontal structure with several

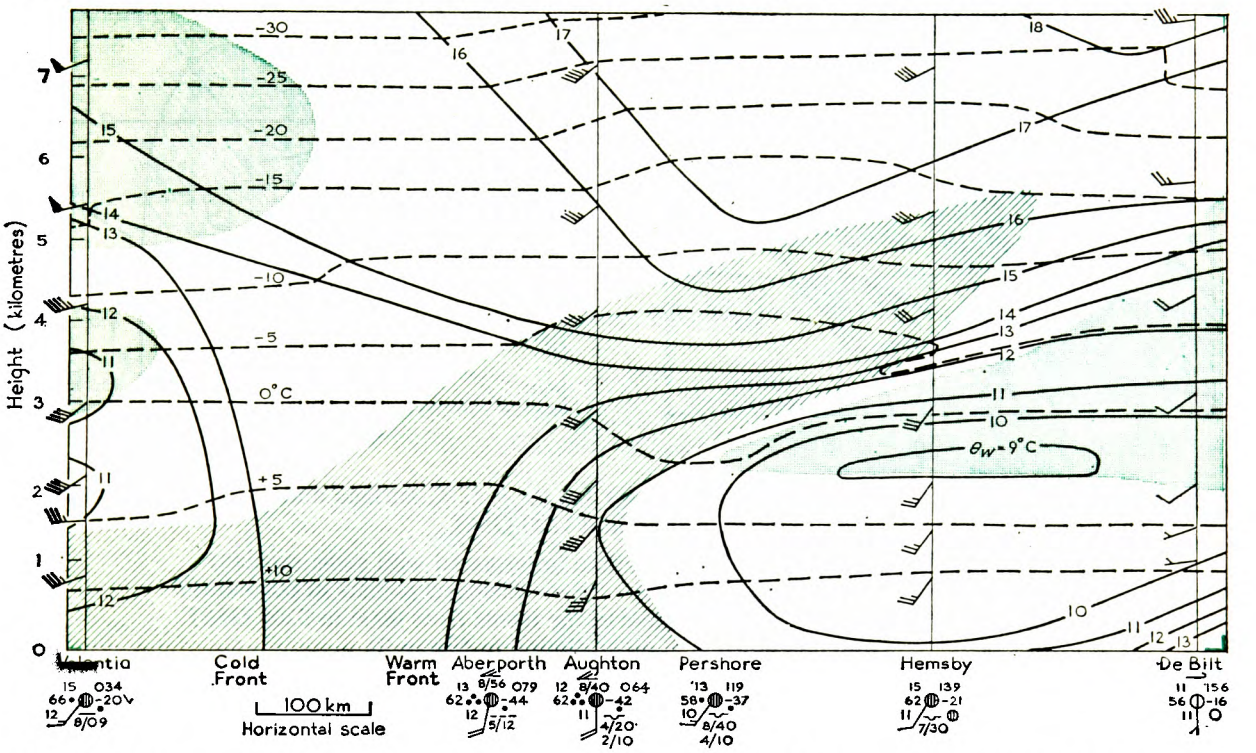

FIGURE 21. 21 August 1965. Cross-section from Valentia to De Bilt (along line AB in Figure 22) at 0000 GMT.

——— Wet-bulb potential temperature (°C) – – – Isotherms (°C)

Green diagonally-hatched area denotes dew-point depression <2·5 degC; green stippled areas denote depression >10 degC. Actual winds are shown.

The system was in an approximately steady state and data from other times (not shown) were incorporated in the analysis. Note the complicated structure over England where several comparatively stable 'frontal' layers are apparent.

frontal zones (identified by a horizontal temperature gradient and an increase in θ_w gradient). There was also a warmer subsided layer around 2·5 km beneath the main frontal zone. The rain was not continuous at Pershore and radar measurements were confined to one period between 0040 and 0155, corresponding to the passage of the eastern belt of rainfall maximum shown on Figure 22.

The relative-flow θ_w surface representative of the low-level front (Figure 22(*a*)) shows a moist southerly flow, relative to the front, centred on the Irish Sea, with ascending air over

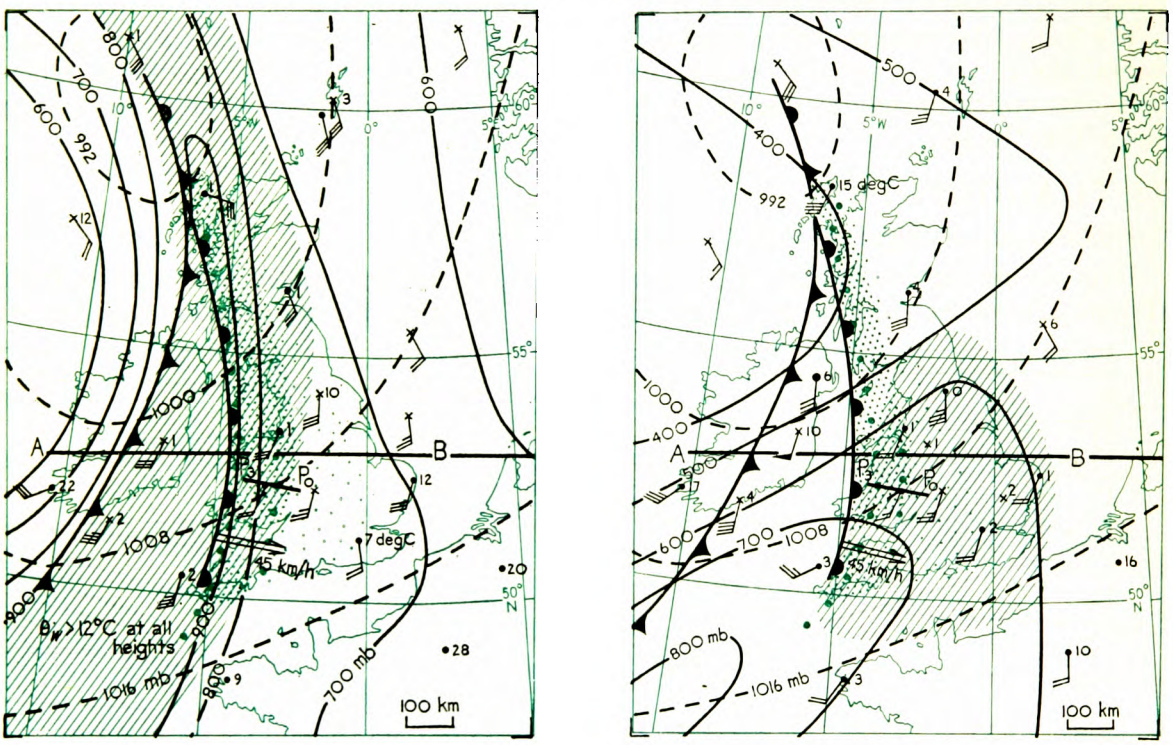

FIGURE 22. 21 August 1965. Relative-flow charts for (*a*) θ_w = 12°C surface and (*b*) θ_w = 15°C surface between 0000 and 1200 GMT.

. 0000 GMT data x 1200 GMT data (interpreted with some caution)
——— Isobars on isentropic surface - - - Sea-level isobars at 0000 GMT
P_0———P_3 Position of radar relative to the fronts from 0000 to 0300 GMT
AB Part of line of cross-section in Figure 21
Surface fronts at 0000 GMT, in usual notation

Green diagonally-hatched areas denote dew-point depression <3 degC on the isentropic surface (values are plotted to the right of data position). Heavy green stippling shows the extent of continuous moderate or heavy rain at the ground at 0000 GMT, light stippling the extent of slight rain. Rainfall maxima at 0000 GMT are denoted by large green dots; maxima could be traced over several hours as they crossed the country. Winds are relative to the movement (290° 45 km/h) of the synoptic pattern.

(*a*) θ_w = 12°C surface

The chart is representative of the lower frontal zones shown in Figure 21. Note that the 1000-mb isobar (not shown) is practically coincident with the 900 mb.

(*b*) θ_w = 15°C surface

The chart, which is representative of a frontal zone in the middle troposphere, shows ascent of moist air over eastern England. Very dry air at lower levels prevented any rain reaching the ground in this region.

Wales and northern England. In the Pershore area the vertical velocity increased to about 5×10^{-3} mb/s on the $\theta_w = 12°C$ surface by 0300 GMT. The $\theta_w = 15°C$ surface (Figure 22(*b*)) indicates a maximum ascent in the Pershore area of about 6×10^{-3} mb/s. There is ascent of moist air up this surface over eastern England but dry air at low levels presumably prevented any surface precipitation. Ascent was more marked on the $\theta_w = 17°C$ surface (not shown) reaching about 10^{-2} mb/s over Pershore.

Horizontal wind field (Figure 23)

The increase in shear at about 2 km is probably coincident with the base of the lowest frontal zone (Figure 21). It is not possible to identify an upper limit to this zone in either Figure 21 or 23. The largest wind shear was in the layer below 0·7 km. The shears indicate warm advection at 2 km and cold advection at 4 km. This decreasing stability probably resulted in the heavier outbreaks of rain that occurred 12 hours later over East Anglia.

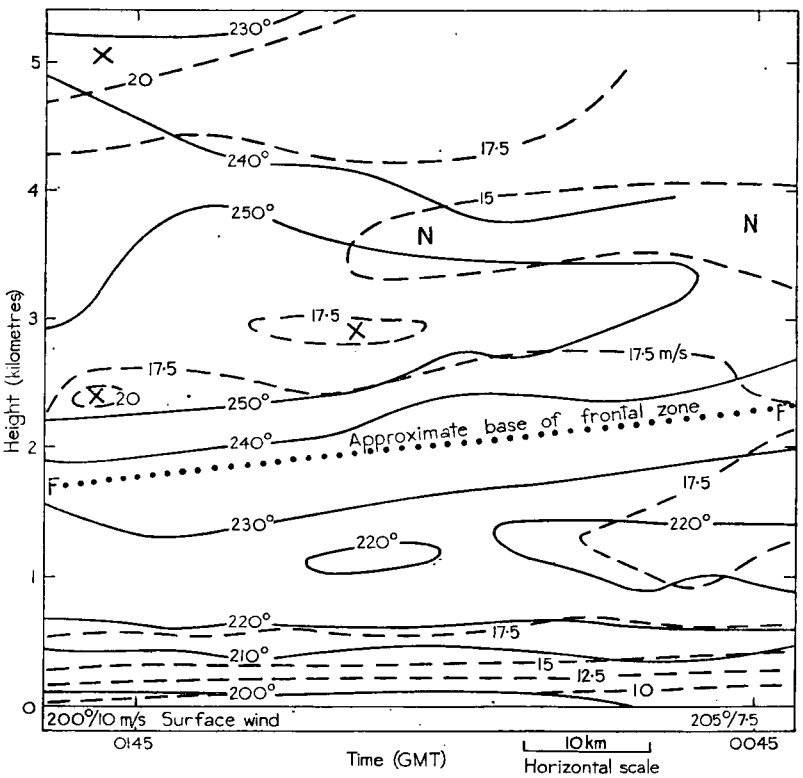

FIGURE 23. 21 August 1965. Height–time section of wind field over Pershore.

——— Direction isopleths - - - Speed isopleths
X Denotes speed maximum N Denotes speed minimum
F . . . . F Base of frontal zone, deduced from synoptic data

The horizontal scale is based on the assumption that the synoptic pattern was moving at 45 km/h. Pershore surface winds are shown at the foot of the diagram.

Divergence field (Figure 24).

In spite of the patchy character of the precipitation as seen on an RHI radar, possibly indicative of a small-scale convective structure, and the variable vertical velocity (see next

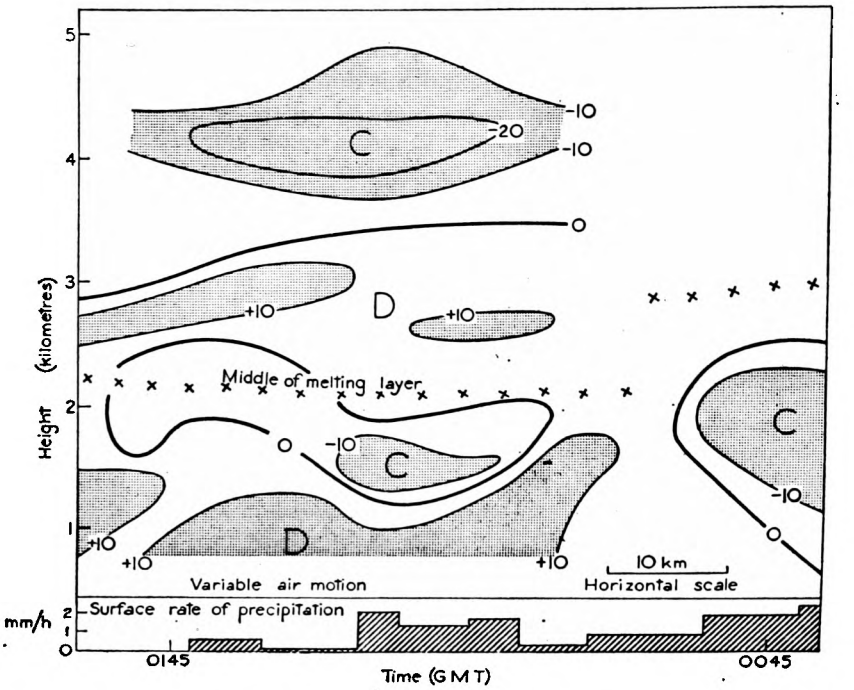

FIGURE 24. 21 August 1965. Height–time distribution of divergence.

C Denotes convergence D Denotes divergence
Regions of $|D| > 10 \times 10^{-5}$/s are shaded

section), persistent layers of convergence and divergence were identifiable. Isopleths at intervals of 10×10^{-5}/s have been drawn with little difficulty in spite of the larger probable errors (because of the variable vertical air motion) compared with other occasions. Divergence predominated below 3·2 km, although an irregular layer of convergence was apparent near 2 km. Air motion in the upper part of the echo was convergent throughout. Surface rainfall maxima correlate well with an increase in convergence near the melting layer.

Vertical air motion (Figures 25, 26)

Vertical velocities obtained from the divergence measurements were calculated relative to the top (at about 2·5 km) of the melting layer (Figure 25). The means over two 15-minute periods were in good agreement with each other and showed relative ascent of 10^{-2} mb/s at 5 km. This was probably an overestimate of the true ascent since the data obtained with the aerial vertical showed some descent at times immediately above the melting layer. There was vertical air motion in the rain throughout the observations. Between 0040 and 0053 an updraught (Figure 26) reached 1 m/s but after 0058 there was continuous downdraught which exceeded 2 m/s at times (shown by the presence of raindrops falling at 11 m/s). A downdraught in snow at 0150 also reached 1 m/s, and was followed by the cessation of the rain at the ground about 10 minutes later. The maximum rate of rainfall occurred at the time of the strongest downdraught in the rain.

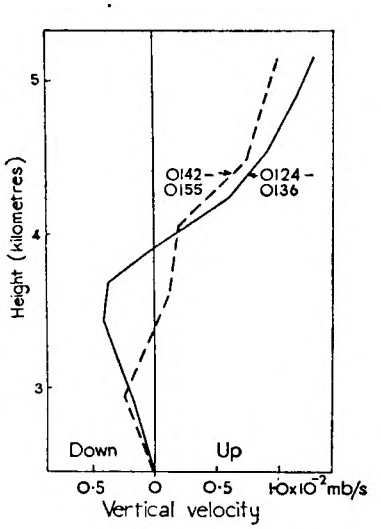

FIGURE 25. 21 August 1965. Vertical velocities deduced from Figure 24.

Data are meaned over the periods 0124–36 and 0142–55 GMT, and the velocities are relative to those at 2·5 km.

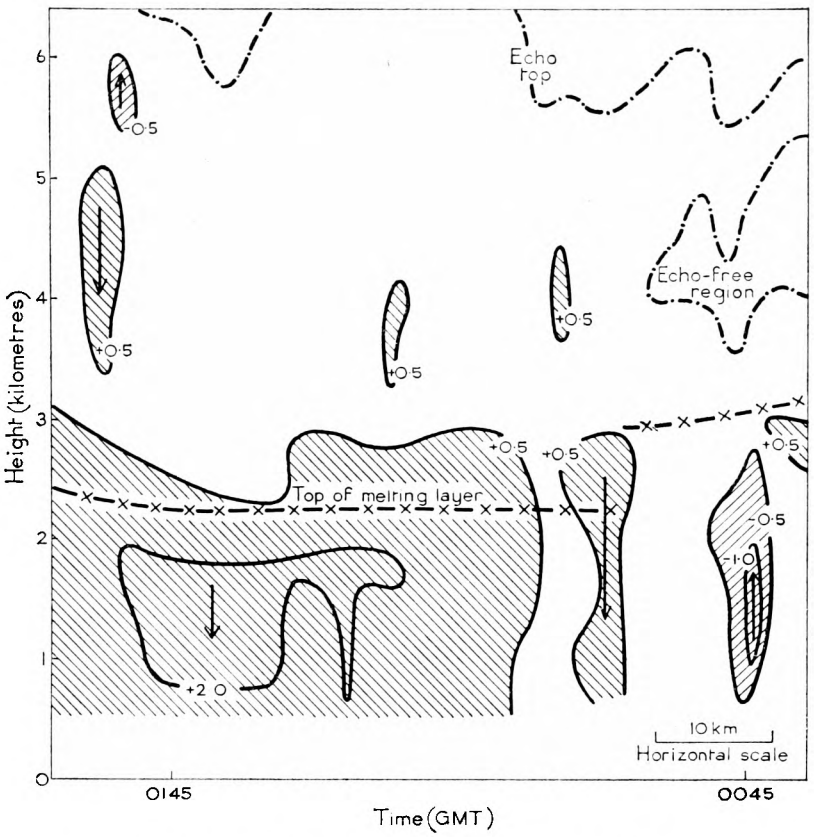

FIGURE 26. 21 August 1965. Height–time section of vertical velocity deduced from measurements taken with the radar aerial vertical.

– · – · Echo top

Regions of identifiable vertical air motion >0·5 m/s are shaded, and arrows indicate the direction of motion. Note the discontinuity in the top of the melting layer at 0057½ GMT, coinciding with the onset of a downdraught.

Discussion of 21 *August* 1965

The rain in which radar measurements were made was less steady than in the other case studies and only lasted for an hour, although there were other periods of rain which were not recorded.

The base of the frontal zone was probably coincident with an increase in the wind shear at 2 km (Figure 23) but the front was not a sharp discontinuity and there were no large wind variations across it. The θ_w analysis showed ascent increasing from 10^{-3} mb/s at 2·5 km to 10^{-2} mb/s at 5 km. This is larger than the values observed; in fact at 2·5 km (Figure 26) downward motion predominated. There were, then, differences between the air motion within the rainbelt, and that on the larger scale. It is not possible to state whether this downward motion was a local topographical feature or part of a mesoscale structure independent of topography.

A remarkable feature of this occasion was the sudden drop in the melting layer at 0057½ (Figure 26). Successive photographs taken when the radar was pointing vertically show that

the fall from 3 km to 2·2 km occurred within 20 seconds. Since snow would only fall about 20 metres in this time the change must have been advected over the radar and it can be confidently interpreted as a spatial discontinuity. It was not accompanied by any marked change in the horizontal wind (Figure 23). Referring to the cross-section (Figure 21) it can be seen that the 0°C isotherm is shown as falling by about 0·8 km in the Pershore area; it would appear that what is shown as a gradual change on this figure was in fact a discontinuity. On the cross-section the change occurs at the edge of a layer of subsided air, the 0°C isotherm being raised by the subsidence (e.g. over Hemsby). The radar data suggest that there was in fact a very sharp mesoscale front separating the subsided air from the moister air to the west. A possible explanation of this feature is as follows. The discontinuity occurred at the time the base of stronger echo aloft extended down to the 0°C level, and thence to the ground. If the air beneath the 0°C isotherm was initially nearly isothermal a small increase in cooling by evaporation from this heavier precipitation may have been sufficient to lower the melting level by several hundred metres. Thus, provided that the stronger echo was aligned in such a way that the wind relative to its movement was parallel to the orientation of its edge, i.e. air was not moving from stronger to weaker echo, a persistent discontinuity in the melting level would be present at the leading edge of the stronger echo. This would be advected with the precipitation.

3.6. 29 NOVEMBER 1965

Synoptic situation (Figures 27, 28)

A cold frontal trough developed over the British Isles during 29 November 1965. Radar measurements were made during intermittent sleet (mixed rain and snow) and snow in the

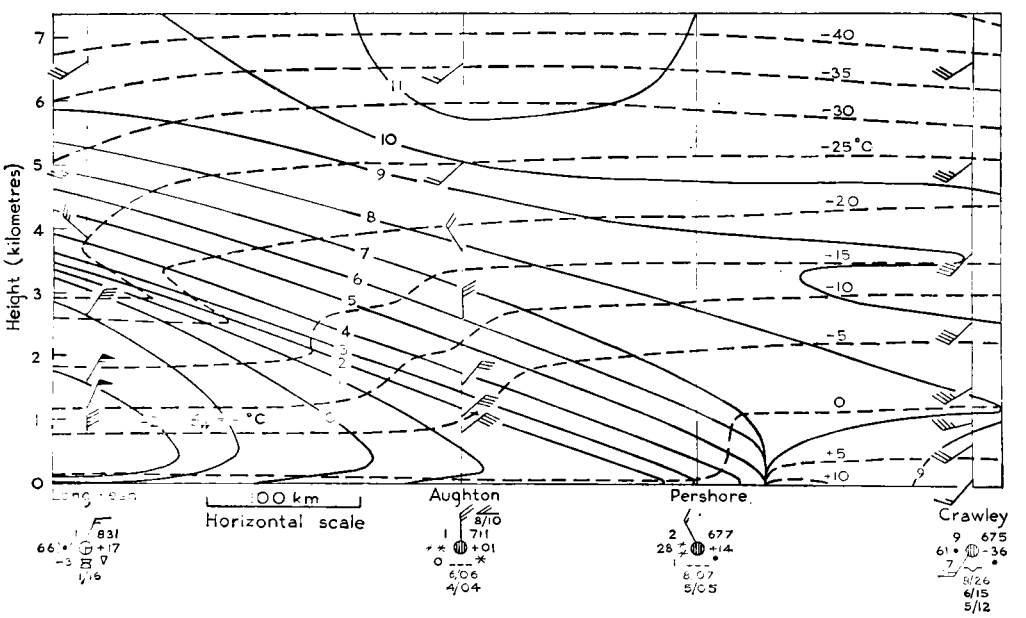

FIGURE 27. 29 November 1965. Cross-section from Long Kesh to Crawley (along line AB in Figure 28) at 1200 GMT.

——— Wet-bulb potential temperature (°C) - - - Isotherms (°C)

The dew-point depression (not shown) was <5 degC at all heights at and between Aughton and Crawley and >5 degC at all heights over Long Kesh. Actual winds are shown.

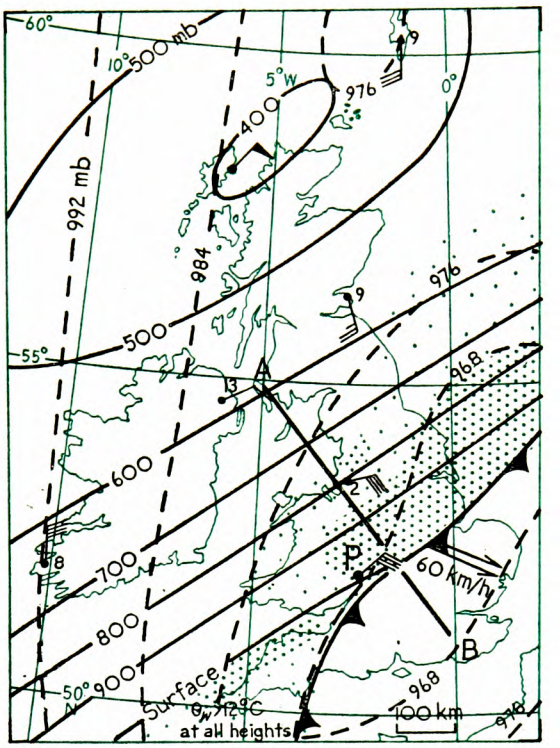

FIGURE 28. 29 November 1965. Relative flow chart for $\theta_w = 4°C$ surface at 1200 GMT.

. 1200 GMT data

——— Isobars on isentropic surface – – – Sea-level isobars at 1200 GMT

P Pershore AB Line of cross-section in Figure 27

Surface front at 1200 GMT, in usual notation

Data for one time only are shown because development was occurring, hence the paucity of data.

Dew-point depressions are plotted to the right of the data position. Heavy green stippling shows the extent of continuous precipitation at the ground, light stippling the extent of intermittent precipitation. Winds are relative to the movement (290° 60 km/h) of the cold front. The relative winds may not represent trajectories in this case although they probably serve as a guide to the large-scale vertical air motion.

cold air behind the surface front (Figure 27). This case is of interest in that it is the only study of a cold front, but it has the disadvantage that it was not possible to assume a steady state even over the three hours of the radar observations.

The relative-flow θ_w chart (Figure 28) shows ascent up the frontal surface over the eastern portion of the map and descent to the west. These conclusions were verified by analyses of θ surfaces (not shown) for 1200 (29th) and 0000 (30th) GMT. Pershore was close to the transition zone, with ascent of, at most, 5×10^{-3} mb/s.

Figure 29 shows the numerically computed mean vertical velocity in the layer 1000–600 mb. (Because the Meteorological Office was in the process of changing computers at the time of this project, this was the only case for which a numerical chart was available.) The motions are computed over a 250-km grid in the region of the British Isles; the model does not include

moisture (Bull[14]), so the figure gives only the broad-scale pattern of the air motion. It can be seen that there is general agreement with the θ_w analysis in that there is ascent over east England and the North Sea and descent to the west, although the transition zone is further east than in Figure 28. This may be because Figure 29 is a mean over a considerable depth of the atmosphere; it may also reflect the lack of moisture in the model.

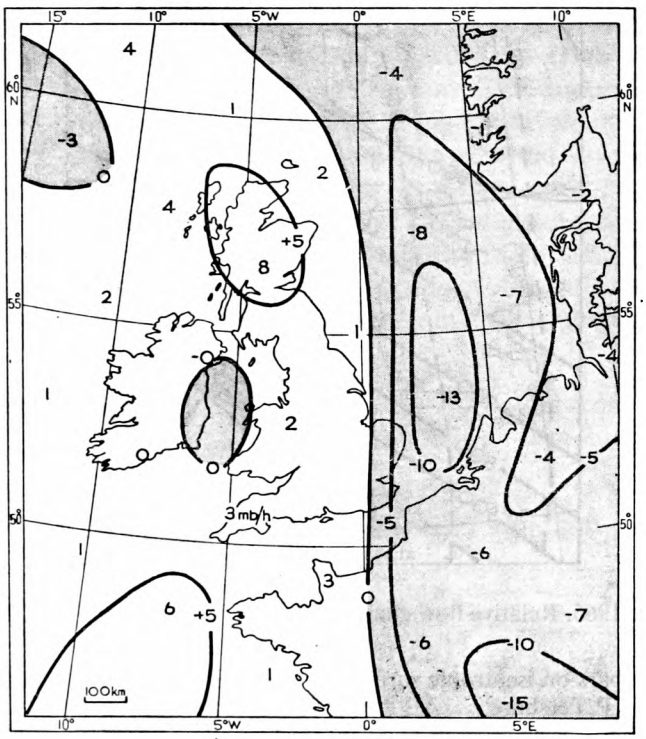

FIGURE 29. 29 November 1965. Numerical computation of the mean 1000–600 mb vertical velocity at 1200 GMT.

——— Isopleths of vertical velocity (mb/h)

Areas of ascending air are shaded. 1 mb/h $\simeq 0{\cdot}28 \times 10^{-3}$ mb/s

Horizontal wind field (Figure 30)

There was considerable variation in the height–time section; a marked shear zone centred at 2 km at 1300 GMT was ascending with time. This corresponded to the frontal zone. There were also persistent, although shallow, layers of maximum and minimum wind speed.

Divergence field (Figure 31)

Convergence predominated below about 2 km, and there was divergence within the frontal zone. The slope of the isopleths shows a tendency to lie parallel to the slope of the shear zone. The presence of divergence within the frontal zone was surprising since synoptically the front appeared to be developing at this time.

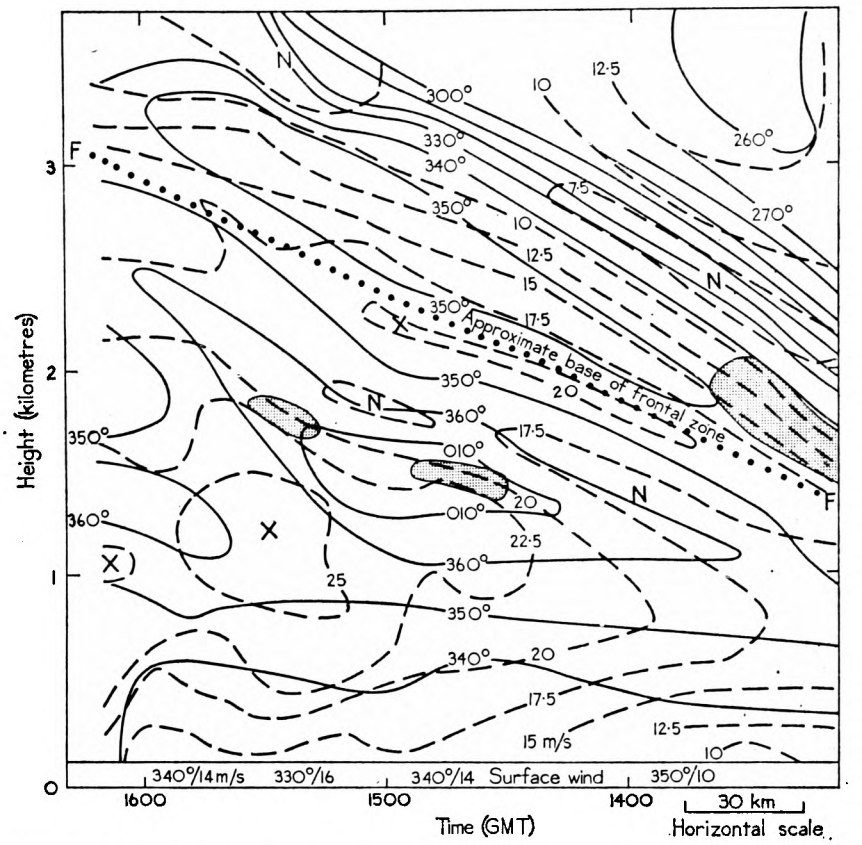

FIGURE 30. 29 November 1965. Height–time section of wind field over Pershore.

——— Direction isopleths - - - Speed isopleths
X Denotes speed maximum N Denotes speed minimum
F . . . F Base of frontal zone, deduced from synoptic data

The horizontal scale is based on the assumption that the cold front was moving at 60 km/h. Pershore surface winds are shown at the foot of the diagram.

Areas of $Ri < 1$ (see Section 4) are shaded.

Vertical velocity (Figure 32)

At the beginning of the period both upward and downward motion were indicated with the aerial vertical, but later identifiable downdraughts were very limited in height and time, whilst there was considerable indication of upward motion, especially at the lower altitudes.

Velocities computed from the divergence measurements were in general agreement with Figure 32 but are not shown since the figure alone provides an adequate picture of the vertical air motion.

Discussion of 29 November 1965

The radar measurements were made during a three-hour period of intermittent sleet and snow. Detectable echo did not extend above 4 km although the synoptic data showed moisture to a much greater height. It is probable that the echo top was determined by the limited radar sensitivity, rather than being a true top to the precipitation.

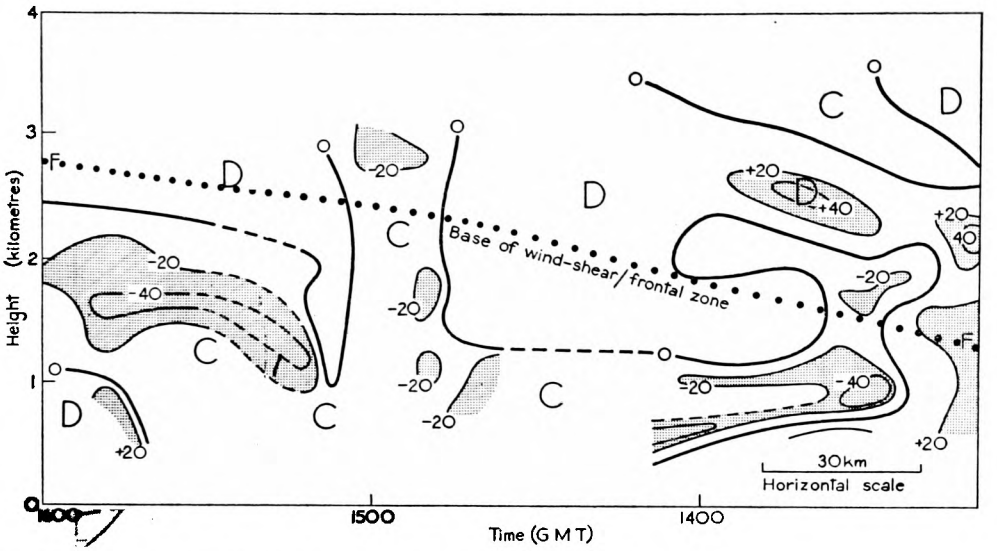

FIGURE 31. 29 November 1965. Height–time distribution of divergence.

C Denotes convergence D Denotes divergence

F .... F Base of frontal zone, deduced from synoptic data and from wind shears shown in Figure 30

Regions of $|D| > 20 \times 10^{-5}$/s are shaded

The rate of rainfall was negligible throughout the period and is not shown.

In view of the persistent ascent of about 0·5 m/s of apparently (on the synoptic scale) moist air, it is surprising that the surface precipitation was so light, being barely indicated by the rate-of-rainfall recorder. If it is assumed that there is no storage of precipitation, a 4 km depth of saturated air ascending at 0·5 m/s would produce rainfall of about 10 mm/h. The heaviest rate observed was only 0·2 mm/h; this coincided in time with the mid-level downdraught at 1340 (Figure 32). It must be concluded that ascent of this magnitude was not widespread.

Below about 2 km the horizontal wind, relative to the surface front, was approximately at an angle of 45° to the height–time section (assuming this also represents a spatial section). Consequently it is not possible to construct a three-dimensional flow diagram (for example similar to Figure 9), but some conclusions as to the three-dimensional airflow can be drawn. During the first hour of observations there were downdraughts of between 0·75 and 1·5 m/s and the horizontal wind relative to the front was about 25 m/s. Consequently during this period the relative trajectory sloped at about 1 in 30 whereas synoptically the front was horizontal in the direction of the relative wind (e.g. Figure 28). This implies either that there was localized motion through the base of the frontal inversion or that there were considerable mesoscale fluctuations in the frontal surface.

The relative-flow θ_w analysis (Figure 28) gave no indication of the vertical velocities in excess of 0·5 m/s (as in Figure 32), so in this instance the θ_w analysis only indicates at most the large-scale flow. Also the 1000–600 mb (surface to 4·2 km) numerical velocities (Figure 29) differ not only in magnitude but also in sign from those measured by the radar, so that this computation did not give any indication of the air motion in the Pershore area.

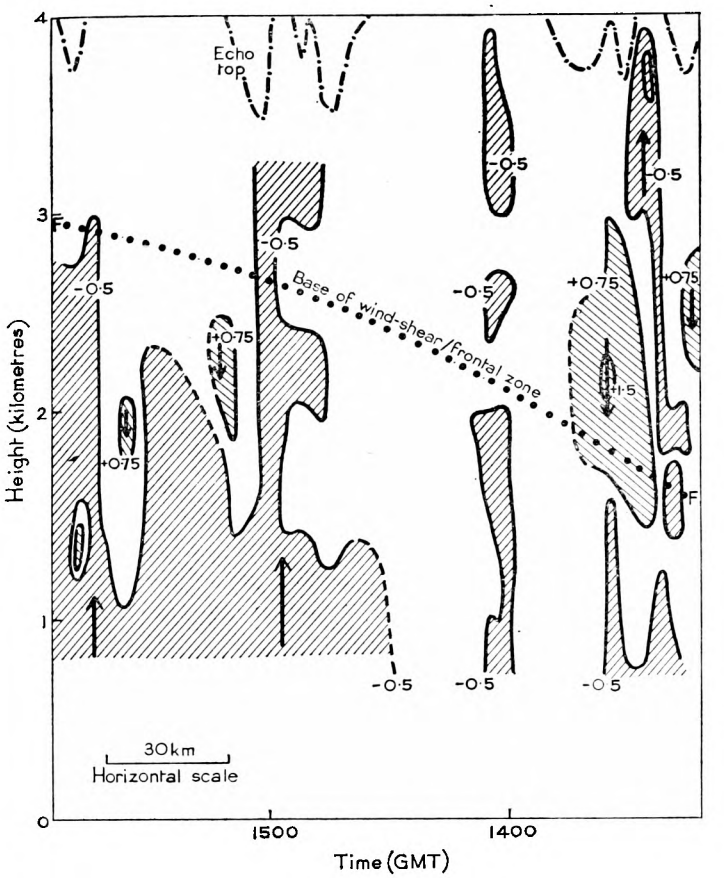

FIGURE 32. 29 November 1965. Height–time section of vertical velocity deduced from measurements taken with the radar aerial vertical.

F . . . . F Base of frontal zone

Regions of identifiable vertical air motion >0·5 m/s upward and >0·75 m/s downward are shaded, and arrows indicate the direction of motion.

3.6. 16 JUNE 1965

Synoptic situation (Figures 33, 34 (*a*) and (*b*))

A small, but deep, depression over the Brest Peninsula at 1200 GMT moved along the north coast of France to be over Holland at 0000 GMT on the 17th. During this period a col crossed southern England. Pershore was just within the area of frontal precipitation, the edge being about 50 km to the north. Air beneath the front showed some sign of instability (e.g. θ_w decreasing with height in Figure 33) but the radar showed little evidence of small-scale convection. The relative-flow chart for θ_w = 12°C (Figure 34(*a*)), representative of the upper surface of the front, shows ascent over Pershore during the observations; this was about 10^{-2} mb/s at 1500 GMT, and decreased with time. A similar pattern occurred on the θ = 20°C surface (Figure 34(*b*)) although the vertical velocities over Pershore were negligible on this surface. The rain ceased when ascent was replaced by descent on the θ_w = 12°C surface.

The synoptic pattern has many similarities to the previous case study, although the relative position of Pershore is different.

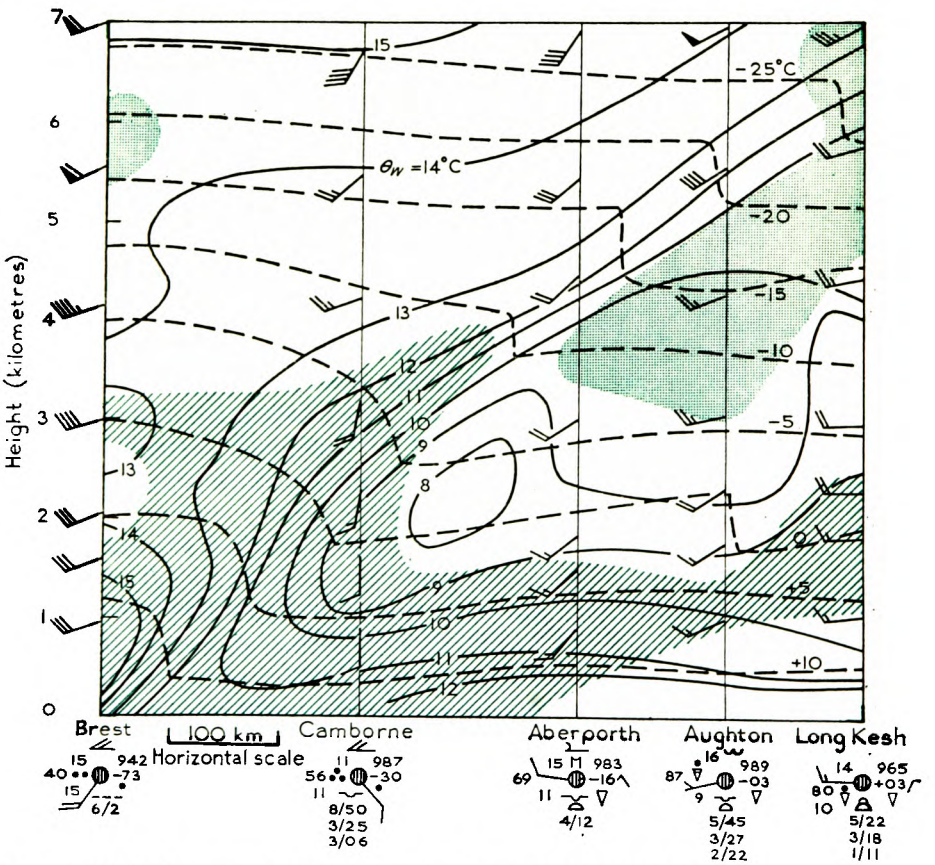

FIGURE 33. 16 June 1965. Cross-section from Brest to Long Kesh at 1200 GMT.

——— Wet-bulb potential temperature (°C) – – – Isotherms (°C)

Green diagonally-hatched area denotes dew-point depression <2·5 degC; green stippled areas denote depression >10 degC. The position of Pershore at 1600 is close to the position of Aberporth in the cross-section. Actual winds are shown.

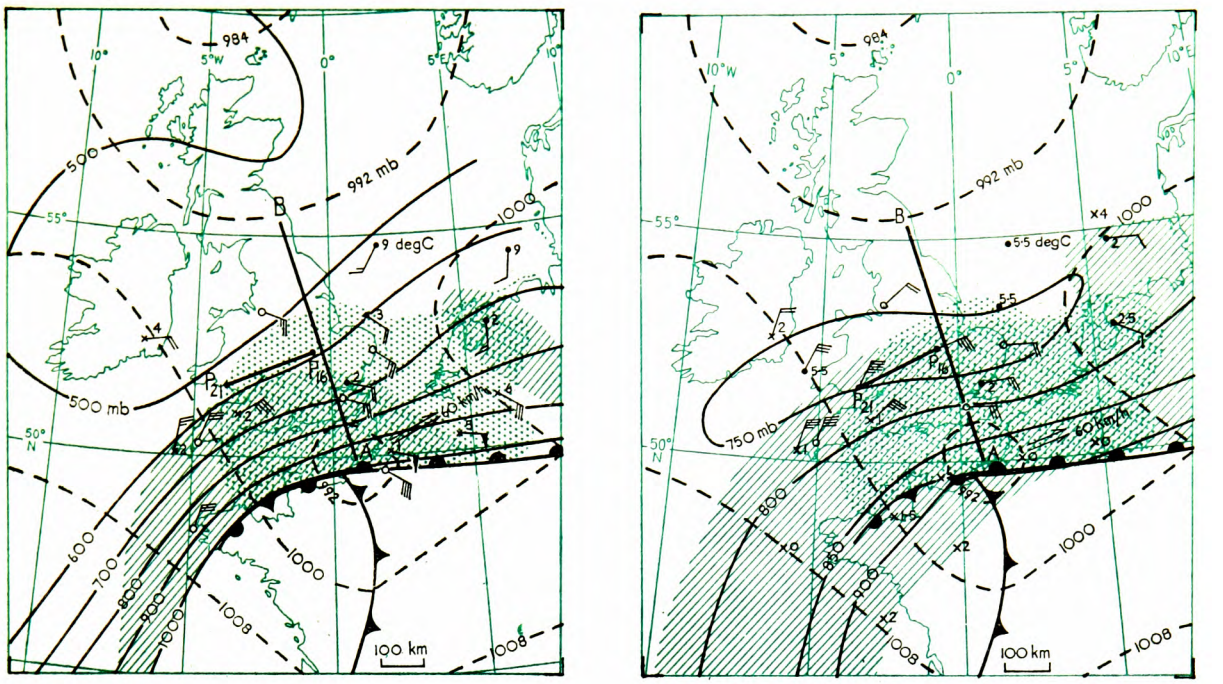

(*a*) (*b*)

FIGURE 34. 16 June 1965. Relative-flow chart for (*a*) $\theta_w = 12$°C surface and (*b*) $\theta = 20$°C surface between 1200 and 0000 GMT on 17th.

. 1200 GMT data o 1800 GMT data x 0000 GMT (on 17th) data
——— Isobars on isentropic surface - - - Sea-level isobars at 1800 GMT
P_{16}———P_{12} Position of radar relative to the fronts from 1600 to 2100 GMT
AB Relative position at 1800 of line of cross-section in Figure 33
Surface fronts at 1800 GMT, in usual notation

Green diagonally-hatched areas denote dew-point depression <2·5 degC on the isentropic surface (values are plotted to right of data position); green stippling shows the extent of rain at the ground. Winds are relative to the movement (245° 60 km/h) of the synoptic pattern. The position of the British Isles is relative to the system at 1800 GMT.

(*a*) $\theta_w = 12$°C surface

The chart is representative of the frontal zone. Note that the western edge of the rain coincides with the edge of the ascending air.

(*b*) $\theta = 20$°C surface

Potential temperature rather than θ_w has been analysed because of the complicated structure of θ_w at these levels (see Figure 33). The chart is representative of the airflow beneath the front over southern England.

Horizontal wind field (Figure 35)

Considerable variations of wind occurred during the observations, associated with the replacement of two cols by north-westerlies at all heights. The figure clearly shows mesoscale features with a detail that probably has not been observed by more conventional means of measuring wind. The centre of the surface col passed about 50 km south-south-east of Pershore at about 1630 and at this time the radar reveals calm winds from 1 to 1·7 km and from 2·5 to 3·0 km, with the strongest winds close to the surface. There were several marked zones of direction shear, although the vector change was mostly small because of the small velocities. At 1600 a change of 90° occurred between 1·5 and 2·5 km and at 1730 there was a change of 120° between 1 and 1·5 km. This latter feature extended to the ground, but with a

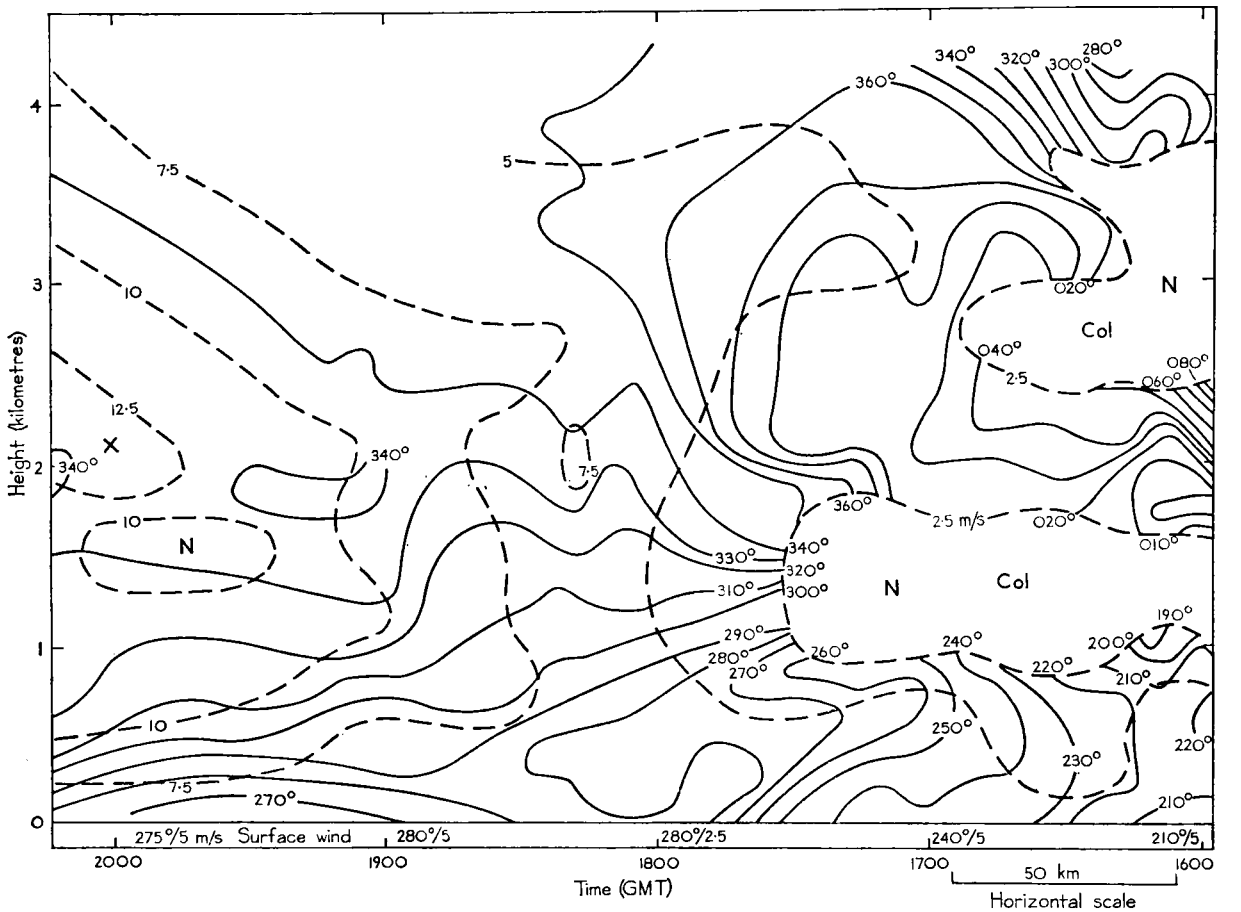

FIGURE 35. 16 June 1965. Height–time section of wind field over Pershore.

——— Direction isopleths - - - Speed isopleths

X Denotes speed maximum N Denotes speed minimum

Direction isopleths are omitted where the speed is less than 2·5 m/s.

The horizontal scale is based on the assumption that the synoptic pattern was moving at 60 km/h. Pershore surface winds are shown at the foot of the diagram.

lessening of gradient, after 2000. The shear zone above 3·5 km at 1600 was probably related to the frontal inversion (Figure 33).

Divergence field (Figure 36)

Divergence predominated in the echo around Pershore, although there were two persistent layers of convergence, one centred at 2·5 km, the other at 1·3 km. These two layers initially were at the height of the two col regions and were associated with the steady increase in the wind speed to the west of these features; thus more air entered the circle of observation than left it. A lowering of the upper convergent layer after 1800 was parallel (on Figure 36) to the lowering of an overhead fallstreak. This is interesting since a fallstreak implies only a mesoscale vertical air motion at the generating level; it is not necessary to postulate small-scale air motion at lower levels—in fact such air motion might tend to diffuse the fallstreak. But it seems that the fallstreak in this case may have been a cause of the variations near 2 km, that is to say the airflow was affected by the presence of the precipitation.

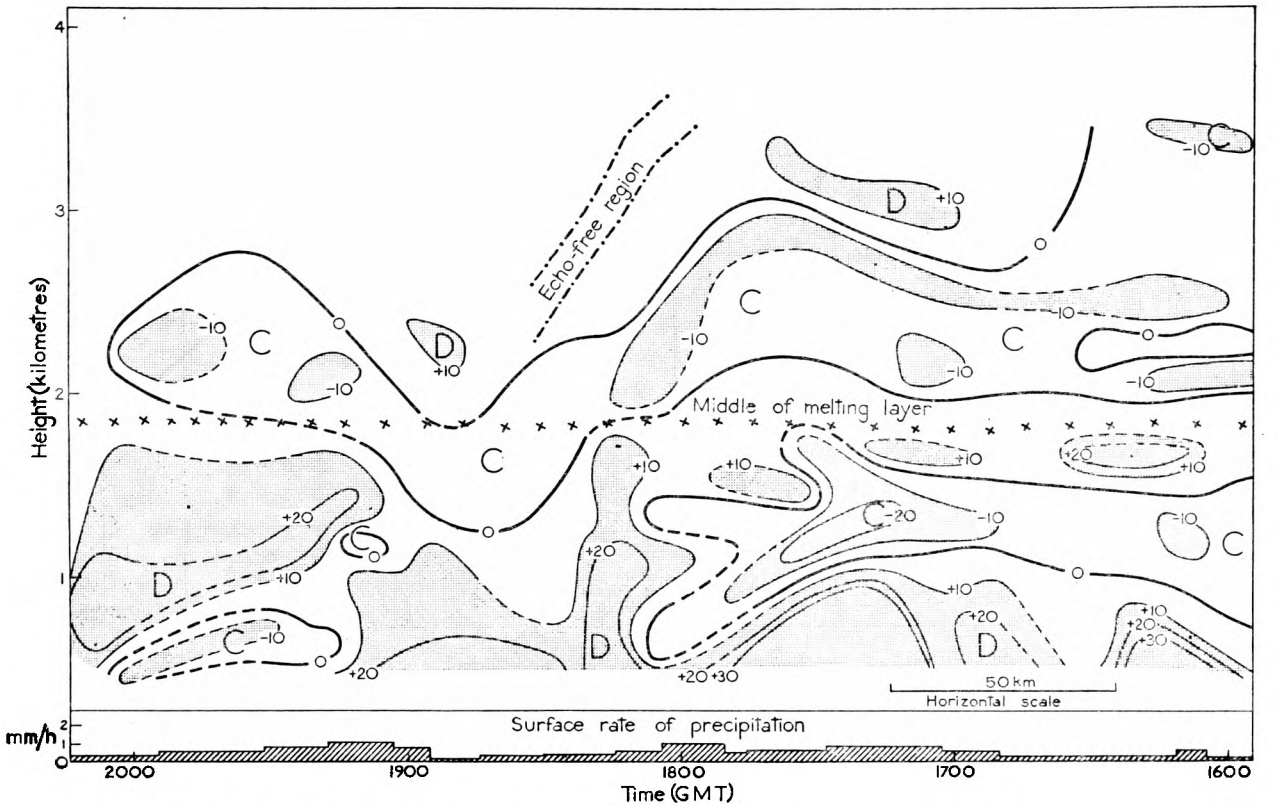

FIGURE 36. 16 June 1965. Height–time distribution of divergence.

C Denotes convergence D Denotes divergence
Regions of $|D| > 10 \times 10^{-5}$/s are shaded

The boundary of a 'fallstreak' of no echo overhead around 1815 GMT is shown. Apart from this feature, overhead echo extended to above 5 km throughout the observations.

Vertical velocity (Figure 37)

Motion was generally downward relative to that at 800 m at all levels up to about 2·8 km. The trend of the lowest levels of the profiles, together with the low-level divergence values (not included in the analysis because of their large probable error) suggests a downward velocity of about $0{\cdot}5 \times 10^{-2}$ mb/s at 800 m. This being the case, air motion was zero until about 1830 at about 3½ km, which corresponds approximately to the base of the frontal zone. By 2000, when the rain ceased, downward motion extended up to at least 3½ km.

Air motion detected by the vertically pointing aerial was negligible. This is in general agreement with Figure 37, the magnitude of the downdraughts at most times being less than is resolvable with the aerial vertical.

Discussion of 16 *June* 1965

The radar observations were made at the edge of an area of frontal rain. The θ_w analysis shows a cause of this rain to be the ascent of moist air up the frontal surface. This ascent, together with the water content of the air at these levels, was sufficient to account for all

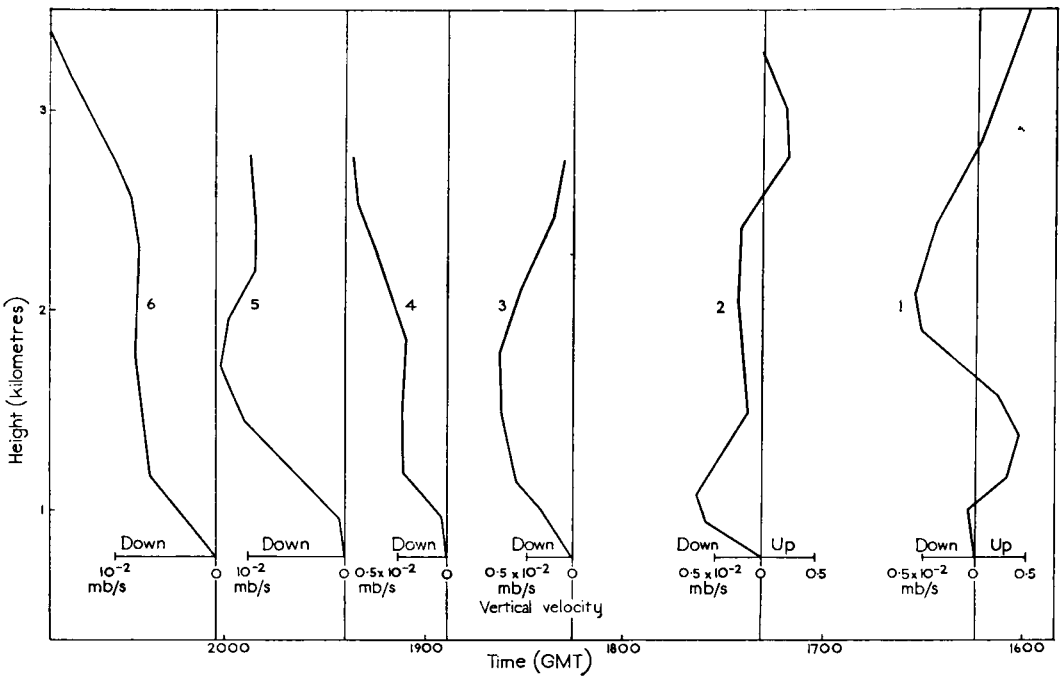

FIGURE 37. 16 June 1965. Vertical velocities deduced from Figure 35.

Data are meaned over a 15-minute period centred on (1) 1618, (2) 1722, (3) 1817, (4) 1852, (5) 1922, and (6) 2008 GMT, and the velocities are relative to those at 800 m. Downward vertical motion predominates.

of the observed rate of rainfall. Consequently the deduction from the radar observations that there was no ascent, and therefore no significant formation of precipitation, below 2·8 km was not incompatible with the occurrence of rain. It can be concluded that, except where the low-level air was dry enough to cause significant evaporation, conditions beneath the frontal surface were irrelevant to the formation of precipitation.

4. COMPARISON OF CASE STUDIES

4.1. *Horizontal wind field*

Radar measurements of the horizontal wind extended into well-marked frontal zones on four (Figures 5, 12, 18, 30) of the six cases presented here, the exceptions being 16 June 1965, when the front was above the maximum height of the observations, and 21 August 1965, when the front was diffuse. There was some consistency in the wind variations across the fronts on different days in that a speed minimum occurred within the frontal zone in all four cases. A speed maximum occurred beneath (Figures 5, 18) or at the base of (Figures 12, 30) the fronts. This is in contrast to the previous case study (Harrold[4]), when a speed maximum was present within the frontal shear zone. The few wind measurements above fronts (Figures 12, 30) showed smaller variations than at lower altitudes.

As would be expected, the winds veered from the surface upwards to about 1 km, the only exception during 26 hours of observations (including Harrold[4]) being a 2-hour period on 9 April 1965 (Figure 12). The reason for this rather persistent anomaly, implying cold advection where it would not have been expected, is not known.

The data have been analysed to determine whether the maximum observed shear can be predicted from routine synoptic observations. In Table II the maximum wind shear observed over Pershore is compared with the changes across the fronts deduced from radiosonde ascents (especially the analysed cross-sections). In four of the six cases the maximum wind shear was similar to that expected from the synoptic cross-section, in two further cases it was about 40 per cent more than this. The table shows that there is little correlation between the maximum vertical wind shear over the circle of Doppler observations and the synoptic-scale

TABLE 2. *Comparison between the frontal wind change and the synoptic-scale frontal intensity estimated from the cross-sections*

Date	1 Doppler-observed maximum vertical shear (ΔV) over 0·5 km *m/s*	2 Doppler-derived Richardson number, *Ri*	3 Synoptic-scale vertical shear over 0·5 km *m/s*	4 Maximum horizontal temperature change over 50 km *degC*	5 Maximum vertical gradient of θ_w ($\Delta\theta_w$) *degC/0·5 km*
20 Jan. 1965	13	1·5	(12)	(5·0)	(3·0)
9 Apr. 1965	14	0·5	10	1·25	2·5
13 Nov. 1964	6	1·5	6	1·75	1·5
21 Aug. 1965	6	3·0	5	0·66	(2·0)
29 Nov. 1965	10	0·7	11	3·0	2·0
1 June 1964	14	0·7	10	1·25	2·5

Brackets enclose uncertain values. On 16 June the front was not reached.

horizontal temperature gradient within the frontal zone, implying either a lack of geostrophic balance or a mesoscale temperature gradient over Pershore different from that on the synoptic scale. There are indications of a relationship of the form $\Delta V \simeq 5\Delta\theta_w$, where ΔV is the vector wind change (column 1) and $\Delta\theta_w$ is the maximum change in θ_w over a height interval of 0·5 km (column 5). That is, the vertical gradient of θ_w within a frontal zone gave a good indication of the maximum observed wind shear. There seems to be no theoretical justification for this deduction, which is based on five studies.

Few small-scale (tens of kilometres) wind fluctuations were observed. The height–time sections generally showed steady variations with time (see especially Figure 30), that is, most features on the mesoscale were also present on the larger scale. Table II includes values of the Richardson number, *Ri*, at the time of the maximum observed shear, where

$$Ri = \frac{g}{\theta}\frac{\partial\theta}{\partial z}\Big/\left(\frac{\partial u}{\partial z}\right)^2.$$

The term $\partial u/\partial z$ was taken directly from the radar observations so that it is a mean over the circle of observation at any one height, and $(1/\theta)(\partial\theta/\partial z)$ was estimated from the synoptic data. Although some error in $(1/\theta)(\partial\theta/\partial z)$ is likely, it is not considered to be serious. The maximum wind shears occurred within the frontal zones and the most stable part of nearby ascents was considered representative of the structure over Pershore. Any errors in the values of *Ri* would be such that the value quoted is probably an overestimate. The table shows that on three occasions *Ri* was < 1. Closer examination of the data (e.g. shaded portions of Figure 30) shows that $Ri < 1$ persisted on occasions over about a 0·5-km layer for more than

30 minutes. A value of $Ri < 1$ is often taken to indicate the likelihood of turbulence but variations in vertical air motion at these times were no greater and the horizontal flow was not more variable over distances of a few kilometres than at other times, as is shown for example by the isopleths in Figure 30. This finding, together with the general lack of any marked variations in the height–time sections of horizontal wind, is in contrast to the results of a similar study by Boucher *et alii*[15] in Massachusetts. They observed periodic breakdowns of a strong wind shear following the occurrence of a layer with $Ri < 1$, resulting in wind changes at any one height of as much as 10 m/s over half an hour.

4.2. *Divergence field*

Divergence measurements were made only when variations in precipitation fall-speed were small over several minutes, so they are representative of only one type of frontal precipitation. With this limitation in mind some general conclusions can be drawn.

The divergence (D) pattern is more complicated than the wind pattern, with small-scale features being common, but persistent layers of divergence and convergence are readily identifiable. These layers are generally horizontal (e.g. Figures 21, 29), and assuming a translation of the pattern over the radar, persist over tens and sometimes hundreds of kilometres. Within a layer, persistent D of 40×10^{-5}/s may occur over a 150-m height interval but the layers are generally shallow and D meaned over a height of 1·5 km is usually an order of magnitude smaller. The simple 'classical' model of low-level convergence and high-level divergence was rarely observed.

Generally, small-scale variations of D did not appear to be related to any features of the precipitation overhead; an exception to this is in Figure 36, where the slope of the pattern is parallel to a fallstreak. It may be that other variations were in fact related to the precipitation structure, but insufficient quantitative radar intensities prevented this from being detected.

4.3. *Vertical air motion*

The Doppler radar has been used to estimate vertical air motion using two separate techniques. When the precipitation was steady, that is to say when variations in the overhead fall-speed were less than about 0·3 m/s over about 10 minutes, the vertical velocity was calculated from the measurements of divergence. Vertical air motion was generally averaged over several aerial rotations, that is over tens of minutes. An example of the shape of the sampled volume is given in Figure 2. An alternative way of estimating vertical air motion was to point the aerial vertically to determine the fall-speed of the precipitation and assume a free-fall velocity. The difference between the two values gave an estimate of the vertical velocity. Air motions in excess of 0·5 m/s (snow) or 0·75 m/s (rain) could be determined in this way. In this second method the sampled volume is a function of the beam width and pulse length. It is $2{\cdot}5 \times 10^5$ m^3 at 2 km range. These two separate techniques enabled vertical velocity to be estimated during most of the Doppler record of precipitation.

Beneath about 3 km, downward motion predominated in four of the seven (including 1 June 1964, Harrold[4]) cases analysed. These four included all three cases when fronts approached from the west, the most usual synoptic situation over Britain. The relative-flow θ_w charts, together with the very limited radar data at higher levels, indicated that there was generally ascent above the frontal surface. Typically, then, the precipitation formed almost entirely in the middle or upper troposphere above the frontal surface. Downward motion beneath the front excluded the possibility of any further growth, except perhaps within the melting layer.

The predominance of downward motion in rain is in keeping with the findings of Caton[10] at Pershore and Harper[16] at East Hill (about 100 km east of Pershore) that there is negligible precipitation growth beneath the melting layer in frontal rain. Also, theoretical calculations using simplified frontal models have shown that downward motion is to be expected in the cold air beneath a frontal zone, e.g. Sawyer.[17] Consequently there is ample evidence that the predominance of downward motion in the radar observations is not incompatible with the occurrence of continuous rain.

On three occasions (20 January 1965, 29 November 1965 and 1 June 1964) ascent, rather than descent, occurred beneath the frontal zone. All three occasions were comparatively uncommon synoptic situations. The large-scale synoptic pattern was studied to determine whether there were any features common only to these three occasions. In particular the stability beneath the front, the advection of low-level vorticity and the isallobaric gradients were studied, but there was no apparent relation between these quantities and the observed air motion. However, there was apparently a connexion with wind at low levels. On days of predominantly downward motion the winds at about 200 m were 190° 8 m/s (9 April 1965), 210° 12 (13 November 1964), 200° 8 (21 August 1965) and light westerly (16 June 1965) whereas on days when ascent predominated they were 130° 10 (20 January 1965), 330° 11 (29 November 1965) and 070° 10 (1 June 1964). It can be seen that predominantly downward motion occurred when the wind was between south and west, but never when it was from other directions. The results from only seven studies are of course insufficient to inspire much confidence in this correlation, but it does suggest that topography may be important in determining the vertical air motion beneath fronts at Pershore. It is not possible to state whether the local (within 10 km say) or the larger-scale topography is the more important, but the similarity of precipitation totals over the west Midlands suggests that the main topographical influence may be the Welsh mountains. Alternatively there may be synoptic differences between fronts with south-westerly winds and other fronts.

Downward motion in excess of 1 m/s was observed for about 10 per cent of the time during which Doppler observations were being made, and in the vast majority of the observations it was confined to the region beneath the melting layer. On three occasions (9 April 1965, Figure 13; 21 August 1965, Figure 26; and 1 June 1964, Harrold[4]) there was a marked discontinuity of vertical velocity over a height interval of about 300 m at the melting layer, with downdraughts of at most 0·25 m/s immediately above, implying a divergence of 3×10^{-3}/s. This suggests that some mechanism within the melting layer was either producing or accentuating downdraughts. A possible explanation is that in steady rain an isothermal layer forms near 0°C and this results in an unstable layer immediately below this level (e.g. Brown[18]). Air within the isothermal layer is then unstable to descent and thus produces a downdraught. Evaporation in the rain would help to maintain the air motion. The compensating updraught, which must be present, was not detected, implying either that it was outside the precipitation area or that the region of downdraught was practically stationary.

An alternative explanation of the downdraughts is that they were the direct result of lee-waves or quasi-stationary eddies induced by the several hilly regions to the south-west and west. However, lee-wave theory predicts a maximum wave amplitude within the stable layer, which was in these cases due to a frontal zone, with a falling off at both higher and lower altitudes, whereas the observed downdraughts cut off sharply at the melting layer, with generally negligible vertical air motion in the snow compared with that in the rain. This sharp cut-off precludes the possibility of the downdraughts being lee waves. On the other

hand it is possible that a quasi-stationary eddy induced by a nearby topographical feature might not extend above the isothermal layer near the 0°C level.

The case studies have shown that the vertical air motion beneath and within a frontal zone can either be steady in time (at one location) and space (assuming a translation of the pattern) or variable with short-period speeds in excess of 1 m/s. It also seems that either one or the other type of motion often persists over several hours and a change-over from one type to the other can be identified. Figure 38 indicates a possible relationship between the height of the base of the front, the mean wind speed beneath the front and the type of vertical air motion. The more variable and larger-magnitude vertical velocities tend to occur when the front is closer to the ground. The results from 9 April suggest that there may be a wind speed below which unsteady motion does not occur.

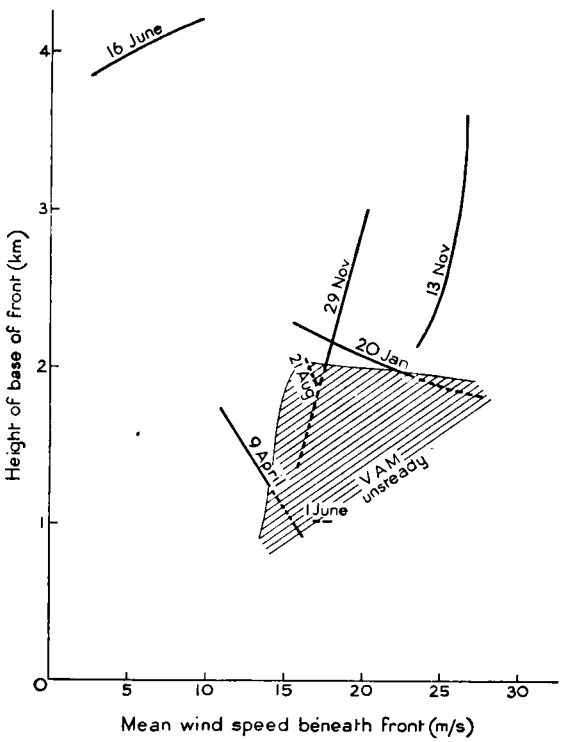

FIGURE 38. Graph showing the relationship between the variability of vertical air motion, the height of the base of the front and the mean wind speed beneath the front, for all seven case studies.

——— Variations in vertical air motion <0·25 m/s
- - - Variations in vertical air motion >0·5 m/s and often 1 m/s

Unsteady vertical air motion, VAM (shaded area), is confined to occasions when the base of the front was below 2 km and the mean wind speed was more than 13 m/s.

A relationship between the thermal structure of the atmosphere beneath the frontal zone and the character of the vertical air motion might also be expected. However, as far as can be judged from radiosonde ascents at stations about 150 km from Pershore, and often outside the precipitation area, the stability at low levels was similar on the different days so this point cannot be investigated.

It has been found that relative-flow θ_w charts give little, if any, indication of the large-scale vertical air motion beneath fronts, although they clearly show the horizontal flow. This is probably because the sparse data do not permit an accurate estimate of the isobar orientation (see, for example, Section 2.4.). Within and above a front such charts generally give the sign and an estimate of the magnitude of the vertical velocity, and this magnitude bears some relation to that observed with the Doppler radar when the vertical air motion is steady, although the observed values are often about twice as large. As would be expected the θ_w analysis gives no indication of the localized motions approaching 1 m/s.

In all of the cases studied the precipitation was slight, rarely exceeding 2 mm/h and usually being less than 1 mm/h. The heaviest rainfall generally occurred during a downdraught beneath the melting layer. Variations in the slight rainfall rates could not be related to any variations in the divergence pattern or to the vertical velocity, but this is not surprising since these small-scale variations probably originated outside the height–time section of the Doppler observations.

5. CONCLUSION

This paper has presented the results of measurements of air motion in frontal precipitation both on the synoptic and smaller scales. The synoptic-scale motion was studied using relative-flow charts of constant wet-bulb potential temperature (θ_w), and these clearly show the presence of moist, often ascending, streams of air in frontal regions. Observed mesoscale variations in the horizontal wind generally were not large. For example, in four (possibly five) of the seven case studies the maximum wind shear observed in the frontal zone as it passed overhead was the same as that deduced from an analysis of routine radiosonde data—the nearest radiosonde station being about 150 kilometres from the radar. In the other two cases the maximum shear was 40 per cent greater than that expected from the radiosonde ascents.

There was, on the other hand, a considerable mesoscale structure of vertical air motion. It appears that the vertical air motion beneath and within frontal zones can be either steady, showing only small (a few centimetres per second) variations, or variable with short-period speeds exceeding 1 m/s. There appears to be a tendency for the more variable air motion to occur when the frontal zone is at a low altitude. It has also been found that in fronts moving from the west, the most usual frontal situation in Britain, the air beneath the frontal zones is descending, and almost all of the precipitation is forming in the middle or upper troposphere, in or above the frontal zone. It is possible that this effect is induced or enhanced by topography.

The comparison between the θ_w charts and the radar results showed that much of the data obtained at Pershore might be considered representative of the precipitation area but it is not possible to state conclusively whether the mesoscale variations are a local feature, perhaps determined by topography, or whether they are typical of frontal structure regardless of locality.

6. ACKNOWLEDGEMENTS

The success in collecting the data reported in this paper is due in large measure to the work of Mr S. R. Smith in maintaining the radar in an operating condition. The authors also thank Mr G. Lowe and Mr D. Membery who did the very tedious task of extracting the initial

data from the photographic record, and Mr E. Finch and Mr D. Carver, vacation students at the Meteorological Research Unit at Malvern, for help in the analysis. The Doppler radar is used by permission of the Director, Royal Radar Establishment, Malvern.

BIBLIOGRAPHY

1. PROBERT-JONES, J. R. and HARPER, W. G.; Vertical air motion in showers as revealed by Doppler radar. *Met. Mag., London*, **91**, 1962, p. 273.
2. LHERMITTE, R. M. and ATLAS, D.; Precipitation motion by pulse Doppler radar. *Proc. 9th Weath. Radar Conf., Boston*, 1961, p. 218.
3. CATON, P. G. F.; Wind measurement by Doppler radar. *Met. Mag., London*, **92**, 1963, p. 213.
4. HARROLD, T. W.; Measurement of horizontal convergence in precipitation using a Doppler radar—a case study. *Q. Jnl R. met. Soc., London*, **92**, 1966, p. 31.
5. BROWNING, K. A. and WEXLER, R.; A determination of kinematic properties of a wind field using Doppler radar. *Jnl appl. Met., Lancaster, Pa.*, **7**, 1968, p. 105.
6. BOYENVAL, E. H.; Echoes from precipitation using pulsed Doppler radar. *Proc. 8th Weath. Radar Conf., Boston*, 1960, p. 57.
7. CATON, P. G. F.; The use of Doppler radar in meteorological research. *Radio electron. Engr, London*, **32**, 1966, p. 46.
8. PROBERT-JONES, J. R.; Meteorological use of pulsed Doppler radar. *Nature, London*, **186**, 1960, p. 271.
9. CATON, P. G. F.; A study of vertical air motion and particle size in showers. *Scient. Pap. met. Off., London*, No. 26, 1967.
10. CATON, P. G. F.; A study of raindrop-size distributions in the free atmosphere. *Q. Jnl R. met. Soc., London*, **92**, 1966, p. 15.
11. GREEN, J. S. A., LUDLAM, F. H. and MCILVEEN, J. F. R.; Isentropic relative-flow analysis and the parcel theory. *Q. Jnl R. met. Soc., London*, **92**, 1966, p. 210.
12. BATTAN, L. J.; Radar meteorology. Chicago, University of Chicago Press, 1959.
13. PETTERSSEN, S.; Weather analysis and forecasting, Vol. I—Motion and motion systems. New York McGraw Hill Book Co. Inc., 1956.
14. BULL, G. A.; Three-parameter atmospheric model used for numerical weather prediction. *Forecasting Techqs Brch Memo., met. Off., London*, No. 9, 1966. Unpublished, copy available in the Meteorological Office Library.
15. BOUCHER, R. J., WEXLER, R., ATLAS, D. and LHERMITTE, R. M.; Mesoscale wind structure revealed by Doppler Radar. *Jnl appl. Met., Boston*, **4**, 1965, p. 590.
16. HARPER, W. G.; Variation with height of rainfall below the melting level. *Q. Jnl R. met. Soc., London*, **83**, 1957, p. 368.
17. SAWYER, J. S.; The vertical circulation at meteorological fronts and its relation to frontogenesis. *Proc. R. Soc., London*, A, **234**, 1956, p. 346.
18. BROWN, E. N.; Observations of the microstructure of a radar bright band and its associated shower. *Tellus, Stockholm*, **16**, 1964, p. 517.

Printed in Scotland for Her Majesty's Stationery Office by David J. Clark Limited.
Dd. 138628 K8 8/68 G521 o/n 303916

© Crown copyright 1968

Published by
HER MAJESTY'S STATIONERY OFFICE

To be purchased from
49 High Holborn, London W.C.1
423 Oxford Street, London W.1
13A Castle Street, Edinburgh 2
109 St. Mary Street, Cardiff CF1 1JW
Brazennose Street, Manchester 2
50 Fairfax Street, Bristol BS1 3DE
258-259 Broad Street, Birmingham 1
7-11 Linenhall Street, Belfast BT2 8AY
or through any bookseller

S.O. Code SBN 11 400044 1